UPPSALA
UNIVERSITET

Digital Comprehensive Summaries of Uppsala Dissertations from the Faculty of Science and Technology 1430

Seismological Investigation of Katla Volcanic System (Iceland)

3D Velocity Structure and Overall Seismicity Pattern

ZEINAB JEDDI

ACTA
UNIVERSITATIS
UPSALIENSIS
UPPSALA
2016

ISSN 1651-6214
ISBN 978-91-554-9696-8
urn:nbn:se:uu:diva-303342

Dissertation presented at Uppsala University to be publicly examined in Axel Hambergsalen, Geocentrum, Villavägen 16, Uppsala, Thursday, 10 November 2016 at 09:00 for the degree of Doctor of Philosophy. The examination will be conducted in English. Faculty examiner: Associate Professor Heidi Soosalu (Leading Seismologist, Geological Survey of Estonia, Tallinn, Estonia).

Abstract
Jeddi, Z. 2016. Seismological Investigation of Katla Volcanic System (Iceland). *3D Velocity Structure and Overall Seismicity Pattern*. *Digital Comprehensive Summaries of Uppsala Dissertations from the Faculty of Science and Technology* 1430. 56 pp. Uppsala: Acta Universitatis Upsaliensis. ISBN 978-91-554-9696-8.

The work in this thesis concentrates on **Katla volcano** in southern Iceland. This is one of Europe's most active volcanoes and its history tells us that it poses many threats to society, both locally (Iceland) and on a broader scale (Europe). Its geological setting is complex, where the effects of a melting anomaly in the mantle and a changing rift geometry, perturb the classical setting of volcanism in a rifting setting.

The work has focused on two aspects. The first is the varying distribution of physical properties in the subsurface around the volcano. The second is the distribution of microearthquakes around the volcano. The physical properties that we study are the speeds of seismic waves that reflect variations of temperature, composition and fracturing of the rocks. These can, therefore, help us learn about long-term processes in the volcano. The seismicity gives shorter-term information about deformation associated with current processes.

I have applied two tomographic techniques to study Katla's subsurface to a depth of 5-10 km, *namely local-earthquake* and *ambient-noise tomography*. The former makes use of the timing of waves generated by local earthquakes to constrain the earthquakes' locations and the distribution of wave speed. Here I have concentrated on compressional waves or P waves with a typical frequency content around 10 Hz. With the latter, surface waves are extracted from microseismic noise that is generated far away at sea and their timing is measured to constrain their wave-speed distribution, which then is used to map shear-wave velocity variations. This is done at a typical frequency of 0.3 Hz. I find that the volcano contains rocks of higher velocity than its surroundings, that Katla's caldera is underlain by low velocities at shallow depth that may be explained by hot or partially molten rocks and that beneath the caldera lies a volume of particularly high velocities that may constitute differentiated cumulates. But, I also find that it is not simple to compare results from such different wave types and discuss a number of complications in that regard.

In addition to the well-known microearthquake distribution in the caldera region of Katla and to its west, we have discovered two additional areas of microearthquake activity on the volcano's flanks, south and east of the caldera. These point to current activity and are, therefore, of interest from a hazard point of view. However, it is difficult to pinpoint their underlying process. Speculation about possible interpretation leads me to hydrothermal processes or small pockets of melt ascending due to their buoyancy or locally enhancing fluid pressure, thereby lowering the effective stress.

Keywords: Volcano tomography, volcano seismicity, Katla volcano, Earthquake location

Zeinab Jeddi, Department of Earth Sciences, Villav. 16, Uppsala University, SE-75236 Uppsala, Sweden.

ISSN 1651-6214
ISBN 978-91-554-9696-8
urn:nbn:se:uu:diva-303342 (http://urn.kb.se/resolve?urn=urn:nbn:se:uu:diva-303342)

Dedicated to those who will
read, use and criticize!

List of Papers

This thesis is based on the following papers, which are referred to in the text by their Roman numerals.

I **Jeddi, Z.,** Tryggvason, A., and Gudmundsson, O., (2016). The Katla volcanic system imaged using local earthquakes recorded with a temporary seismic network. *J. Geophys. Res., Solid Earth (in press).*

II **Jeddi, Z.,** Gudmundsson, O., and Tryggvason, A., (2016). Ambient-noise tomography of Katla volcano, south Iceland, and some ambiguity in its interpretation. Manuscript intended for *J. Volc. Geoth. Res.*.

III Sgattoni, G., **Jeddi, Z.,** Gudmundsson, O., Einarsson, P., Tryggvason, A., Lund, B., and Lucchi, F., (2016). Long-period seismic events with strikingly regular temporal patterns on Katla volcano's south flank (Iceland). *J. Volc. Geoth. Res*., **324,** 28-40.

IV **Jeddi, Z.,** Sgattoni. G., Gudmundsson, O., Tryggvason, A., and Lund, B., (2016). A peculiar cluster of microearthquakes on the eastern flank of Katla volcano, southern Iceland. Manuscript intended for *Jökull.*

Reprints were made with permission from the respective publishers.

Contents

Abbreviations

1-D	One-dimensional
2-D	Two-dimensional
3-D	Three-dimensional
AUB	Austmannsbunga
BSL	Below sea level
DD	Double difference
ENT	Enta
EVZ	Eastern volcanic zone
EVFZ	Eastern volcanic flank zone
FMM	Fast marching method
FMST	Fast marching surface tomography
FTAN	Frequency-time analysis
HF	High frequency
HNM	High noise model
IMO	Icelandic meteorological office
KKE	Kötlukottlur
LET	Local earthquake tomography
LF	Low frequency
LNM	Low noise model
LP	Long period
LSQR	Least squares
MAR	Mid Atlantic ridge
NVZ	Northern volcanic zone
Ö-S	Öreafjajökull-Snæfell
RP	Reykjanes Peninsula
RU	Reykjavik university
SIL	South Iceland Lowland
SISZ	Southern Iceland seismic zone
SNR	Signal to noise ratio
SP	Snæfellsnes
SVD	Singular value decomposition
TFZ	Tjörnes fracture zone
UU	Uppsala university
VT	Volcano tectonic
WVZ	Western volcanic zone

1. Introduction

"Success consists of going from failure to failure without loss of enthusiasm."

Winston Churchill

Volcanoes are among the most complicated as well as interesting features of the Earth. In addition to a general curiosity on the dynamic processes that create volcanoes, the importance of studying a volcano lies in the fact that a volcanic eruption can cause a hazard both locally (e.g., lava flows and flash flooding) and globally (e.g., ash clouds). Many different methods have been developed during the past years to study volcanoes through their history (e.g., geology, petrology) and their current state (e.g., seismic activity, gas emission). Nevertheless, the nature of volcanic eruptions is still unpredictable. Studying the different aspects of an active volcano can comprehensively complete the picture of each individual volcano and its uniqueness, while adding information to the general knowledge about volcanic systems.

Iceland is a region with high volcanic activity. It is characterized by a high rate of basaltic volcanism and a high volume fraction of extrusives in crustal accretion compared to mid-ocean ridges (Pálmason, 1980). It is therefore of major interest to be able to describe the internal structure of the volcanoes in this highly active and complex volcanic area. The unique setting of Icelandic volcanism allows for comparison with the different regions and by contrasting environmental factors (e.g., crustal thickness, topography, and caldera size) we may better understand the volcanic plumbing, i.e., processes of melt ascent and accumulation in the crust. This in turn can help with deciphering the available monitoring information and eventually contribute to the assessment of volcanic hazards.

Subglacial volcanoes, in particular, are more hazardous because of the magma-ice interaction, which may result in explosive eruptions. This was exemplified by the 2010 Eyjafjallajökull summit eruption and the associated jökulhlaup (glacial flood) that caused a major air traffic disruption, despite its mild-explosive character (Einarsson and Hjartardóttir, 2015). The subglacial Katla volcano is located 25 km west of Eyjafjallajökull, and it spans over an area larger than Eyjafjallajökull. In addition, higher eruption frequency and larger eruptions have been reported for Katla in the past compared to the ones for Eyjafjallajökull (e.g., Thordarson and Larsen, 2007). Focusing on the study of the subglacial Katla volcano in southern Iceland, using seismological methods constitutes the basis of this thesis, which was set up in collaboration with the Centre of Natural Disaster Science (CNDS).

The history of a volcano and the processes operating at different depths can be studied by analyzing the previous and present chemical and physical properties of the erupted material. A series of storage regions, at different depths, which are periodically connected by feeding structures with magma transfer from a deep source to the earth's surface, is defined as plumbing system (Caricchi and Blundy, 2015). Different geological analyses in the past focused on retrieving the state of the plumbing system of the Katla volcano, reporting different interpretations, as e.g., a simple plumbing system (Óladóttir et al., 2008) or a persistent shallow- and deep-crustal magma storage (Budd et al., 2016). However, our desired knowledge about the status of a volcano and its plumbing system requires real-time monitoring of the volcano. In this study, we use seismological methods to address the current state of the volcano by imaging seismic velocities and locating the seismic activity. The plumbing system and the active source regions of the volcano can then be discussed based on the results of our modeling. Therefore, the main purpose of the thesis is to shed light on the three-dimensional (3-D) structure of the Katla volcano as well as study the general seismicity pattern in the area.

This work will be presented in the following sections, starting with a description of the geological setting of Iceland (2.1) and more specifically Katla (2.2). The current state of our knowledge about Katla is reviewed in section 3. Section 4 presents the configuration of a dense temporary network, operating between 2011 and 2013, which provided data for this study. Section 5 focuses on the description of the methodology used, local earthquake tomography (5.1.), ambient seismic noise tomography (5.2.), and relative earthquake locations (5.3.). A summary of the four included papers included in the thesis is comprised in section 6, while section 7 concludes on the results and observations. A Swedish summary is provided in section 8.

2. Geological Setting

2.1. Iceland

Iceland is located at the Mid Atlantic Ridge (MAR) that formed due to the opening of the North Atlantic during the Eocene (~24 million years ago (e.g., Sæmundsson, 1978; Oskarsson et al., 1985)) by the drifting apart of the North American and the Eurasian plates. The oceanic spreading leads to an extensional tectonic setting. Iceland emerged above sea level probably due to the excessive amount of magmatic supplies that originate from its underlying mantle plume (e.g., Bjarnason et al., 1996; Wolfe et al., 1997). The crust beneath Iceland has a thickness between 20 and 40 km (Gudmundsson, 2003). The thick crust along with the high rate of melt supply may distinguish the Icelandic volcanism from the mid-ocean ridge volcanism in general (Pálmason, 1980). Furthermore, Iceland was mostly ice-covered during the Pleistocene and today about 11% of the country, including some of the active volcanoes, is still under ice (Björnsson and Pálsson, 2008). The interaction of magma with ice and water is an important feature of volcanism in Iceland. The majority of this volcanism is basaltic (Jakobsson, 1979); however, silicic rocks are found at the active central volcanoes as well as eroded ones in the Tertiary sequence (Pálmason, 1971; Bjarnason et al., 1993). Being host for both mafic and silicic volcanism puts Iceland in the center of the bimodal volcanism debate on the origin of the silicic material (e.g., Carmichael, 1964, Bjarnason, 2008).

The co-existence of the MAR and the mantle plume have formed complex rifting zones in Iceland and the currently active plate boundary consists of a series of volcanic and seismic transform zones that have developed through time (Figure 1). The volcanic zones are divided into two types, the volcanic rift zones, characterized by extensive crustal spreading, and the volcanic flank zones, which are associated with no or little crustal spreading. The MAR cuts Iceland at the Reykjanes Peninsula (RP) in the south-west and then it continues towards the Hengil triple junction where it branches to a) the Western Volcanic Zone (WVZ) towards the north-east and b) the South Iceland Seismic Zone (SISZ) towards the east. At the eastern edge of the SISZ, the rifting zone continues along the Eastern Volcanic Zone (EVZ) in a north-easterly direction until it reaches the northern end of Iceland's biggest glacier, Vatnajökull where the Northern Volcanic Zone (NVZ) propagates towards the north. At the northern coast of Iceland, Tjörnes Fracture Zone

(TFZ) connects the rift back to the MAR. The Snæfellsnes (SP) and Öreafjajökull-Snæfell (Ö-S) are the flank zones towards the west and east, respectively. The spreading rate of the EVZ is decreasing from north to south. Accordingly, the southern end of the EVZ to Vestmannaeyjar is named the Eastern Volcanic Flank Zone (EVFZ) (LaFemina et al., 2005) (Figure 1). These volcanic zones include 35 volcanic systems which typically consist of a central volcano, often with a caldera and an associated fissure swarm (Figure 1).

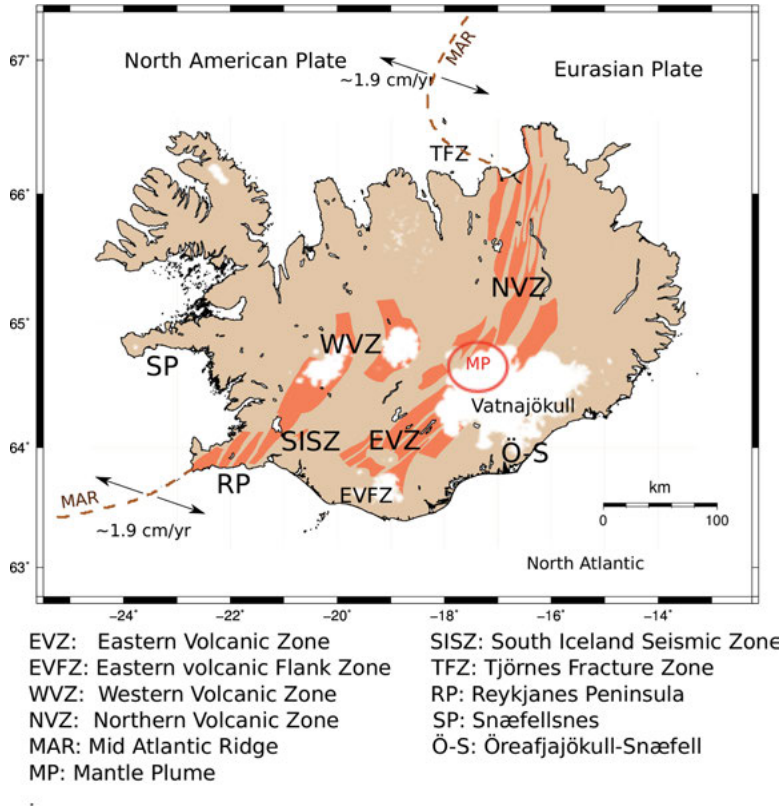

Figure 1. Tectonic setting of Iceland. The North American and the Eurasian plates are spreading approximately ~1.9 cm/yr along the MAR (e.g., DeMets et al., 1994; Sigmundsson, 2006). Volcanic and seismic zones are labeled along Iceland (Einarsson and Sæmundsson, 1987). The Iceland plume (MP) is marked with an open circle at the center of its approximate location underneath the northwestern end of the Vatnajökull glacier (Wolfe et al., 1997).

2.2. Katla Volcanic System

The Katla volcanic system, including the central volcano and its associated fissure swarms, is one of the most active systems on Iceland since hundreds

of thousands of years (Jakobsson, 1979). It is located on the EVFZ, where rifting across it is thought to be insignificant at present time (LaFemina et al., 2005). Katla's central volcano meets the central volcano of Eyjafjallajökull 25 km to the west, while the east-west striking volcanic fissures lie between them (Einarsson and Brandsdóttir, 2000). Its associated fissure swarm, Eldgjá, is distributed about 80 km towards the north-east of the central volcano (Björnsson et al, 2000). Katla has a large summit caldera (~110 km²), which is elongated northwest-southeast (Björnsson et al., 2000) (Figure 2). Silicic explosive eruptions, as the one that has created Sólheimar ignimbrite, could possibly be a reason for the formation of Katla's caldera (e.g., Lacasse et al., 1995).

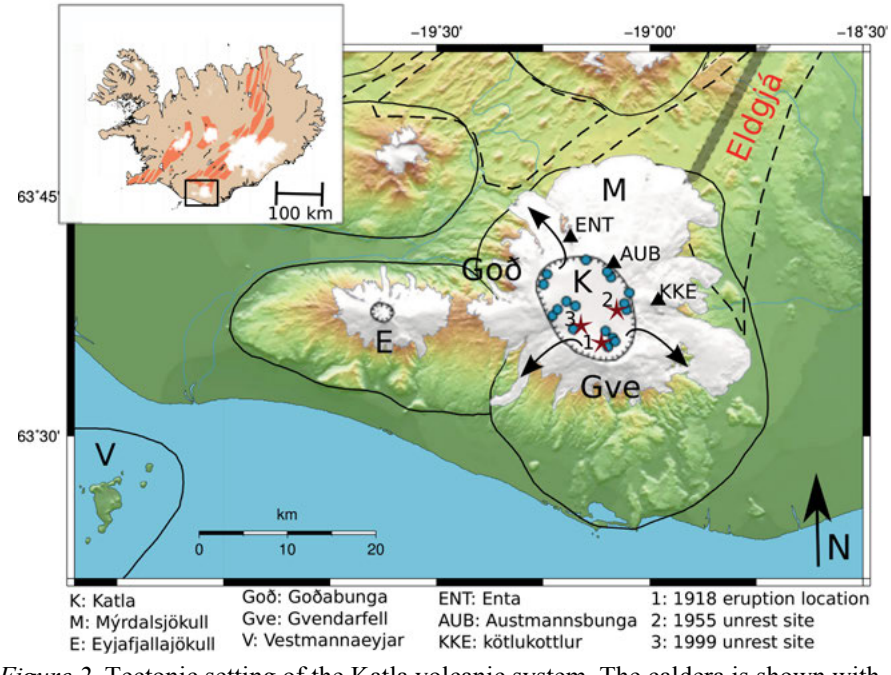

Figure 2. Tectonic setting of the Katla volcanic system. The caldera is shown with the hatched line, the central volcano with a solid line, and the fissure swarm with a dashed line (Einarsson and Sæmundsson, 1987). Triangles refer to nunataks (ice-free exposure) on top of the glacier. Glaciers are white. Pathways for glacial discharge are illustrated with black arrows on the rim of the Katla's caldera. Geothermal cauldrons (depression in the ice surface) on the surface of Mýrdalsjökull glacier are indicated by blue dots (Guðmundsson et al., 2007). The locations of the 1918 eruption, the unrest episodes in 1955 and 1999 are marked with red stars numbered from 1 to 3. The inset in the upper left corner shows the tectonic map of Iceland and includes the study area, which is outlined with the black rectangle.

Most of Katla's eruptions have been originated inside the central volcano with phreatomagmatic behavior (due to magma-ice interaction), while the eruption activity outside might not be as frequent as it is productive. For

example, the Eldgjá fissure eruption in 934-49 A.D. produced the largest known amount of lava (~19 km3) from the Katla volcanic system (Thordarson and Larsen, 2007). Twenty eruptions have been recorded in Katla since 1100 (e.g., Thordarson and Larsen, 2007). The repose time for Katla's eruptions ranges between 13 and 95 years (Larsen, 2000). The last eruption was in 1918 and this 98-year repose time is the longest known in its written history. Nevertheless, Katla was not truly calm during these years and it has shown persistent seismic activity since 1955 (Tryggvason, 1973). Furthermore, several unrest episodes have also been recorded in the volcano, which are summarized in Table 1 and their approximate location are shown in Figure 2.

The Mýrdalsjökull ice-cap covers the caldera including a large part of the central volcano (~600 km²). The ice thickness varies between 10 and 700 m and there are only three rhyolitic nunataks (ice-free exposure) in the glacier, Enta (ENT), Austmannsbunga (AUB), and Kötlukottlur (KKE) (Lacasse et al., 2007) (Figure 2). Localized heat flux beneath sub-glacial volcanoes could cause depression in the ice surface, which is known as cauldron (Björnsson, 1975). Guðmundsson et al. (2007) have reported 17 known cauldron locations on the Mýrdalsjökull glacier using radar altimetry coupled with kinematic GPS (Figure 2). Scharrer et al. (2008) have used a total of 30 synthetic aperture radar (SAR) images within a period of 12 years, starting in 1994, and discovered 6 more cauldron locations in addition to those reported by Guðmundsson et al. (2007). Cauldron locations have been proposed to be related with the bedrock topography of the caldera (Scharrer et al., 2008), although it is still not clear. The accumulated water beneath cauldrons is usually drained in the form of jökulhlaup. The caldera rim is glacially eroded in three main areas, facing northwest, southwest, and southeast, which are providing path ways for the jökulhlaups (Björnsson et al., 2000) (Figure 2).

Table 1. Summary of recorded unrest episodes on Katla since 1955.

Unrest period and possible interpretation	Summary of observations
June 1955 • **Small subglacial eruption (Sturkell and Sigmundsson, 2003)**	• Jökullhlaup from the eastern rim (Kötlujökull) of the Katla caldera (e.g., Thorarinsson, 1975) • Formation of two shallow cauldrons (e.g., Thorarinsson, 1975)
July 1999 • **Small subglacial eruption (Einarsson, 2000)**	• Jökullhlaup from the southwestern rim (Sólheimajökull) of the Katla caldera (Sigurdsson et al., 2000) • Continuous seismic tremor and increased geothermal activity for weeks after the jökullhlaup (Einarsson, 2000; Sigurdsson et al., 2000; Sturkell and Sigmundsson, 2003) • Formation of a new cauldron (Guðmundsson et al., 2007) • Inflation and increased seismic activity in nearby Eyjafjallajökull (e.g., Pedersen and Sigmundsson, 2006)
2001 • **Volcanic intrusive activity (Soosalu et al., 2006)** • **Ice movement (Jónsdóttir et al., 2009)**	• Increased seismicity in the west of Katla (near Goðabunga) (e.g., Einarsson et al., 2005; Soosalu et al., 2006)
July 2011 • **Increased heat release** • **Magma intrusion** • **Minor subglacial eruption** **(Sgattoni, 2016)**	• A jökullhlaup from Kötlujökull • Deepening of some cauldrons • Increased seismicity together with emergence of new source of activity in southern rim of the glacier • Tremor burst for ~23 hours (Sgattoni, 2016 and references therein)

3. Current State of Knowledge on Katla

The Katla volcanic system produces mostly high Fe–Ti basalts of the transitional-alkaline magma bodies (e.g., Jakobsson, 1979) together with a subsidiary volume of felsic magma, which erupts from the central volcano and is exposed as nunataks around the caldera rim (Larsen et al., 2001; Lacasse et al., 2007). During Holocene, Katla's volcanism has been classified accordingly into three categories (Larsen, 1994): 1) explosive basaltic eruptions along volcanic fissures within the caldera; 2) explosive silicic eruptions from vents associated with the caldera, and 3) predominantly effusive basaltic eruptions involving both the central volcano and the fissure swarm, e.g., the Eldgjá fires. The products of Katla's eruption are well documented in the last 1100 years, but the evolution of its plumbing system is still vague. Meyer et al., (1985) suggested the infrequent replenishment of a shallow magma reservoir in the Hekla-Katla area by using petrological and geochemical observations from the Neovolcanic zones of Iceland that results in mixing of magmas of diverse composition. Óladóttir et al. (2008) showed a variable composition of the basaltic tephra layers (e.g., concentration of incompatible elements) with time and suggested that these changes could be explained by three cyclical episodes in the evolution of the plumbing system beneath the Katla volcano: 1) the simple plumbing system with magma traveling directly from a deep reservoir to the vent of the volcano, 2) the plumbing system consisting of multiple sills and dykes, and 3) the shallow crustal magma chamber. According to their model, Katla volcano is currently in a period of a simple plumbing system (Óladóttir et al., 2008). However, a thermobarometry investigation of the basaltic tephra erupted from Katla volcano over the last 8 kyr suggests the existence of persistent shallow- and deep-crustal magma storages beneath Katla (Budd et al., 2016).

Earthquakes in the Mýrdalsjökull area are recorded since the establishment of the Icelandic seismic network in 1988. Einarsson (1991) analyzed the seismic data from the network all over Iceland and described the seismic activity of Katla in two separate clusters: within the caldera and to the west of the caldera, in the Goðabunga region. This seismic activity has exhibited different seasonal characters; the Goðabunga seismic cluster has had a clear annual cycle for decades, with a peak in seismicity in the late autumn, while the caldera has less seasonal variations (Einarsson and Brandsdóttir, 2000). The seismic activity in the Goðabunga region increased in the autumn 2001 and remained high until early 2005 (Sturkell et al., 2008) and consequently

the seasonal character of the Goðabunga seismicity was less obvious during this period (Soosalu et al., 2006). The increased seismic activity of Goðabunga was assumed to be due to either an intruding cryptodome at shallow depths (Soosalu et al., 2006) or ice falls (Jónsdóttir et al., 2009). Since July 2011, the seismicity pattern changed and a new source of activity emerged on the southern rim of the Mýrdalsjökull glacier near Gvendarfell Rise during the unrest episode in the caldera (see Table 1). Furthermore, in the present study a peculiar seismic activity is reported near the eastern rim of the glacier, at the tip of Sandfellsjökull, which was mostly active during December 2011.

GPS measurements on the nunataks near the caldera rim of Katla for the period 1999 to 2004 were analyzed by Sturkell et al. (2008). They modeled their observations using a ~5 km depth point source and interpreted the observed deformation to be due to glacial isostatic adjustment and inflation, respectively. Pinel et al. (2007) worked on data from two continuous GPS stations, between 2000 and 2006. Their modeling also required the assumption of magma inflow to explain the observed horizontal velocities. However, Árnadóttir et al. (2009) suggested that the observed horizontal velocities could be a consequence of rheological structure and fast deglaciation rates. Similarly, Spaans et al. (2015) explained the long-wavelength uplift observed with satellite radar interferometry (INSAR) and GPS measurements from 2001 to 2010 as the response to long-term shrinking of the ice cap.

No inflation was detected in the GPS stations to explain the increased Goðabunga seismic activity in 2001. As the nearby GPS stations were all located north east of Katla and the GPS site closest to the Goðabunga seismic activity was located at a distance of ~8 km, the increased activity was inferred to be due to a very shallow and localized anomaly (Sturkell and Sigmundsson, 2003; Sturkell et al., 2008).

The velocity structure of Katla was modelled in a two-dimensional (2-D) seismic undershooting experiment by Guðmundsson et al., 1994. Four shot points used in their seismic refraction experiment along a profile from the south-southeast to north-northwest, passing through the caldera. The image based on this data set revealed low P wave velocities together with an S wave shadow zone underneath the caldera, which was interpreted as a shallow magma chamber. Reduced P and S wave velocities were also reported in a region of the same dimensions as the caldera using local earthquakes (Jónsdóttir et al., 2007), which were attributed to high temperatures and intense fracturing. However, the sparse seismic network around the volcano resulted in poorly resolved images. Therefore, by deploying a denser network, during a much longer time period, we could potentially improve our understanding of Katla's 3-D structure.

4. Field Work Experiment and Data Acquisition

The permanent seismic network in Iceland, the South Iceland Lowland (SIL) seismic network, started in 1988 as a collaborative project between the Nordic countries on earthquake prediction. Station installation, data acquisition and analysis were planned by the project (Stefansson et al., 1993). The whole network was improved during the following years and the Icelandic Meteorological Office (IMO) currently operates a seismic network including more than 60 stations spread all over Iceland. The first station close to Mýrdalsjökull, MID, started its operation in 1990 and is located to the west of Katla, near Eyjafjallajökull. At the time of the 2010 Eyjafjallajökull eruption; there were 5 stations around Mýrdalsjökull: MID, ESK, SNB, HVO and GOD (Figure 3). Shortly after the eruption, the permanent seismic network of IMO was expanded as 5 new stations were installed in the area. All stations were around Mýrdalsjökull and Eyjafjallajökull, except VES which is located on Heimaey island in Vestmannaeyjar. Even though the number of stations around Katla was doubled in 2010-2011, the stations were not close to the seismic source locations within the caldera. To improve the earthquake locations and in order to have a better understanding of the source and the path effects in the area, a network of nine temporary stations was installed on and near Mýrdalsjökull by Uppsala University (UU) and Reykjavik University (RU), between May 2011 and August 2013. In May 2011, two stations were positioned on the nunataks to the northeast (AUB) and north (ENT) of the caldera. One month later, the eastern nunatak Kötlukottlur, inaccessible until then, was reached and a third station (KKE) was installed on the rim of the caldera. The rest of the stations (six in total) were distributed around the glacier (Figure 3). All stations were deployed by the end of October 2011.

Later, during the summer of 2014, two more stations (GVE and SHR) were installed close to the southern seismic cluster (~1-2 km away) to constrain the epicentral location of the seismic activity there, as the closest station at that time was ~6 km away (GAV). In addition, the GAV station was reinstalled to minimize the effect of network geometry on the estimation of hypocentral location. All of these (three in total) stations were also equipped with GPS. In Figure 3, the locations of the temporary and permanent stations

used in this study are shown. Details regarding the equipment used in each station, including the dates of installation, are summarized in Table 2.

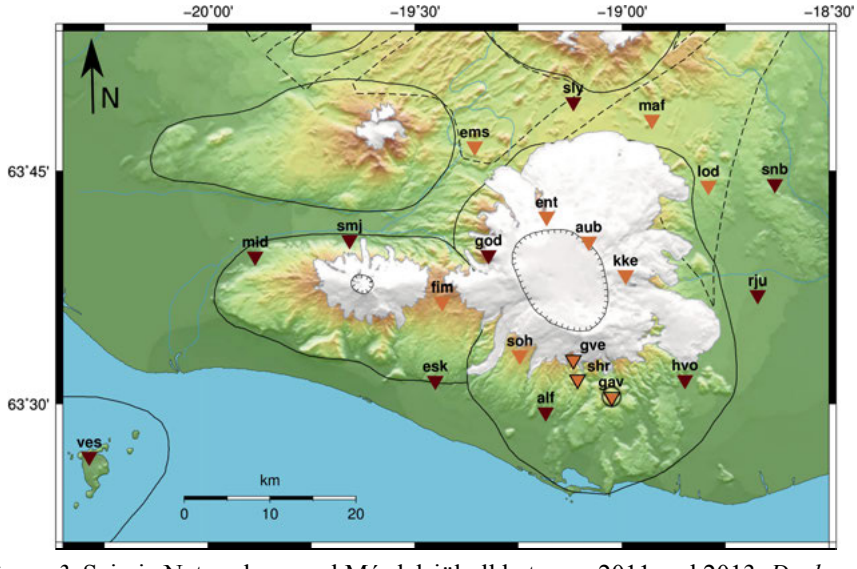

Figure 3. Seimic Network around Mýrdalsjökull between 2011 and 2013. *Dark triangles:* permanent IMO stations. *Light triangles:* temporary UU and RU stations between May2011 and August 2013 (no outline), between July 2014 and August 2014 (black outline). The station, GAV, has been operating on both time periods; black open circle indicates the station.

The location of the temporary stations around the glacier was determined considering a) a distance of ~5 km between the stations, which would densify the permanent network in the area, and b) the potential access to the area. The equipment used in each station was quite heavy; therefore we tried to choose places we could reach by car. Due to the weather conditions in Iceland, especially during the winter, we tried to deploy the seismic sensors in a way that they are not highly affected by wind and water. The measuring sites were chosen on bedrock high enough, compare to their surrounding area, to avoid flooding during the spring, and with sufficient slope, to drain the water from. The sensors were installed directly on bedrock to maximize the ground coupling. Plastic barrels with a waterproof cap approximately one meter high were buried and a small tube at the base of each barrel was used for water drainage. The sensor was set inside the barrel and the cables came out from the bottom of the barrel. Insulation was also used in order to protect the sensors from extreme temperature variations. Finally, rocks were stacked around the part of the barrel reaching above ground (Figure 4). The stations were powered with batteries, wind generators and solar panels. The wind generators and solar panels, together with the GPS, were mounted on a mast

at about 15 m away from the sensor to avoid noise produced by wind generator. The digitizer and batteries were installed in waterproof boxes and usually some rocks were on top of the boxes to avoid any movement due to strong wind. All connecting cables were also buried or covered by rocks.

Table 2. Summary of the information for the seismic network around Mýrdalsjökull.

Station	Sensor	Digitizer	Installation date	Operator
VES	LENNARTZ 5s	GURALP	January 2011	IMO (Permanent stations)
SNB	LENNARTZ 5s	GURALP	April 1993	
SMJ	GURALP CMG-3ESP	GURALP	December 2010	
SLY	GURALP CMG-3ESP	GURALP	May 2011	
RJU	GURALP CMG-3ESP	GURALP	December 2010	
MID	LENNARTZ 1s	GURALP	May 1990	
HVO	LENNARTZ 5s	GURALP	October 1999	
GOD	GURALP CMG-3ESP	GURALP	September 2006	
ESK	LENNARTZ 5s	GURALP	October 2001	
ALF	GURALP CMG-3ESP	GURALP	January 2011	
FIM	GEOTECH KS-2000	REFTEK	September 2011	UU and RU (Temporary stations terminated 15th of August 2013 except AUB)
LOD	LENNARTZ 5s	REFTEK	September 2011	
KKE	LENNARTZ 5s	REFTEK	July 2011	
AUB	LENNARTZ 5s	REFTEK	May 2011	
ENT	LENNARTZ 5s	REFTEK	May 2011	
SOH	GURALP CMG-3T	GURALP	October 2011	
MAF	GURALP CMG-3T	GURALP	July 2011	
EMS	GURALP CMG-3T	GURALP	July 2011	
GAV	GURALP CMG-3T	GURALP	July 2011	
GAV*	GURALP CMG-3T	GURALP	July 2014	UU (Temporary stations terminated at the end of August 2014)
GVE	GURALP CMG-3T	GURALP	July 2014	
SHR	GURALP CMG-3T	GURALP	July 2014	

*station GAV was reinstalled in the summer 2014

The access to many of these temporary stations was limited to a few months per year due to the weather conditions, e.g., snow, strong winds, flood risk. Thus any technical-instrumental problems could not be resolved quickly, which resulted in long station down times. In some cases, the solar panels were found destroyed due to icing problems or flying debris and the wind generators were broken, which lead to occasional failure of the power supply at some stations. Nevertheless, the deployment of the temporary network

during the two years and a half was fairly successful considering the amount of continuous recordings we gathered (see Paper I for detail). In addition, experience from the deployment could potentially improve future network deployments in similar harsh conditions.

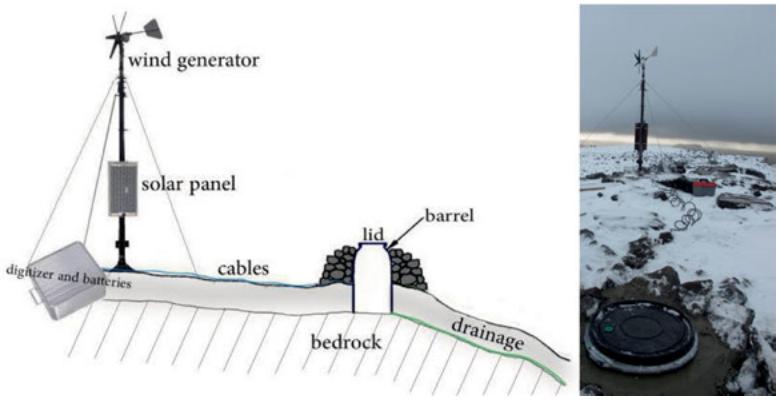

Figure 4. Left: Schematic figure of station setting. *Right:* Site of station SOH. It was installed on the southwest rim of the Mýrdalsjökull glacier in October 2011.

5. Methodologies

Seismic elastic waves represent the most valuable resource for investigating the internal structure and composition of the earth. The waves travel through the earth and carry the information from the deep/shallow interior to the surface. Therefore, the methods based on seismic-wave analysis are quite distinctive among other geosciences. A simple instrument sensitive to up-down motions of the earth records ground motion as a function of time, i.e., seismometer. These recordings (seismograms) can be used for quantitative analysis of seismic waves.

A seismic wave can be released by sudden breaking of rocks or an explosion within the earth that can be natural or man-made. Fluid-like flow, e.g., global convection, magma movement beneath a volcano, can also produce small waves by microearthquakes. In a volcanic system, magma and/or volcanic gases and/ or hydrothermal system fluid movements can either cause rocks to break (discrete source in time and space) or cracks to vibrate (continuous seismic signal). Thus, an active volcano is rarely quiet and microseisms are commonly observed in volcanic regions worldwide. A commonly used classification separates the volcanic events into long-period (LP), volcano tectonic (VT), and hybrid or mixed events (McNutt, 2005). LP events are devoid of high frequency in their frequency spectrum, have an emergent P wave and unclear S wave. Sometimes the S wave is missing. VT events have the appearance of ordinary tectonic earthquakes, have a broad spectrum, sharp P wave onsets and a clear S wave. Hybrid events have characteristics in between the LP and VT events. Additionally, seismic background noise (ambient noise), as a relative persistent vibration on the ground, which can be recorded everywhere on the earth, provides valuable information on the structure of the subsurface, e.g., seismic velocity.

Eventually, continuous monitoring of a volcano could help to reveal a volcano's potential awakening/reawakening. Seismic recordings are unique for each active area and provide information about the current state of a volcano and its plumbing system. For example, estimation of seismic velocities can be a potential diagnostic tool to determine the presence of fluid or gas in the volcanic system and can be used to track magma reservoirs beneath a volcano.

From the abundance of techniques exploring the different types of data, I have used three relevant methods, which focus on studying recorded seismic waves and translate them into the information that can be used to study the

status and structure of the volcano. The methods are explained briefly in the following sub sections.

5.1. Local Earthquake Tomography

Local Earthquake Tomography (LET) is widely used and fairly well-established since it was introduced to earth sciences by Aki (1974). The idea of tomographical methods originates from the medical sciences, where it is used to image the body organs. By using LET, we aim to determine the sub-surface velocity structure for an area within a local seismic network. In this thesis, PStomo_eq (Tryggvason et al., 2002) is used to model the seismic velocity structure beneath the Katla volcano. It inverts simultaneously for P and S wave velocities as well as hypocenter locations using arrival-time data. Here, the general principles of the inversion method are briefly described (see Menke (1986) for details).

The seismic recordings contain the response of the earth, which are produced by the interaction of seismic waves with materials along their traveling paths from the seismic source to the receiver. Property of earthquakes on recorded seismic waves, e.g., amplitude, arrival time, frequency content, could be used to understand the ongoing mechanism at the source as well as properties of the medium that the waves propagated through. The first-arrival times of the body waves are commonly used to estimate the hypocentral location, origin-time and structural properties (e.g., seismic velocities) the waves have travelled through. The LET problem was initially used to solve only for 3-D seismic velocity structures using the first-arrivals, but later the simultaneous inversion for earthquake location parameters and velocity structures was introduced (e.g., Crosson, 1976; Thurber, 1983). There are different ways to solve the coupling between velocity structure and hypocentral parameters. One is by separation of variables that on its introduction in the early 80s made LET feasible as it reduced the size of the matrix that needed to be inverted. More details could be found in Pavlis and Booker (1980) and Thurber (1983) as the methodology is still used today as an important part in linearization (see below) of the problem. In the following paragraphs, the main concepts of LET by means of inversion processes are going to be introduced.

The velocity structure is a continuous medium and the propagation of a seismic wave through such a medium is defined as a line integral along a raypath, which is perpendicular to the propagating wave:

$$d = \int_{t(S(r))} S(r)dl \qquad (1)$$

where d is the time it takes for the seismic wave to travel along the path l between the source and receiver, dl is the differential length of the raypath,

$S(r)$ is the slowness field (the inverse of velocity), and r is the positional vector.

Because the path of a seismic ray depends on the velocity structure, $l(S(r))$, the problem is non-linear. To deal with the nonlinearity of the inverse problem, it needs to be linearized iteratively. Every (linearized) step contains 1) the forward computation of travel paths and times, and 2) the inversion for model slowness perturbations and hypocentral locations to minimize the data misfit. In general, the forward problem formulates as:

(2) $$d = G(m)$$

where G is a forward operator and relates data d (here the arrival time of the observed phases) to model parameters m (here the velocity structure S^{-1} and hypocentral locations $x, y, and\ z$). The predicted data (d^{pre}) are then computed using the given model parameters (m_0) by a finite difference approximation of the Eikonal equation:

(3) $$(\frac{\partial d}{\partial x})^2 + (\frac{\partial d}{\partial y})^2 + (\frac{\partial d}{\partial z})^2 = S^2$$

In step 2, for a set of predicted data the residuals (here the arrival time residuals) are computed as:

(4) $$residual = d^{obs} - d^{pre}$$

The residuals are then used for perturbing the model parameters and, ultimately, the best solution of the inversion scheme is given by a model that minimizes the 'cost' function (Q):

(5) $$Q = \left(d^{obs} - G(m)\right)^T C_d^{-1} \left(d^{obs} - G(m)\right)$$

where $C_d = \sigma^2 I$ is the data covariance matrix, which contains the observational error (σ).

The inverse solver used Least Squares (LSQR), which is a conjugate gradient operator (Paige and Saunders, 1982). The formal model errors for the slowness models are not obtained with an iterative solver like LSQR, and have to be obtained by other means. The hypocentral parameters are solved for using Singular Value Decomposition (SVD) as part of the separation of variables procedure, and the (linear) error estimates of these are therefore obtained.

In addition, the LET problem is a non-unique problem as the observations sample the subsurface structure sparsely. We have no control of where the earthquakes occur and the sensors cannot be placed underground, hence the network configuration and the earthquake locations are the reason for any

lack of information as well as the discretization of the medium to a finite number of cells. Thus, additional information or constraints, such as regularizations, are needed in the inversion process. PStomo_eq adds a set of equations to minimize the Laplacian of the slowness perturbation field of adjacent cells. Subsequently the 'cost' function will be modified to:

$$Q = \left(d^{obs} - G(m)\right)^T C_d^{-1}\left(d^{obs} - G(m)\right) + \text{ƙ}(m^T L^T L m) \quad (6)$$

where L is the Laplacian smoothing operator and ƙ is the weighting parameter controlling the degree of smoothing (Tryggvason et al., 2002). Low weights on the smoothing constraints results in unstable and rough models, even though the data could be fitted successfully. On the other hand, larger weighting parameters will remove all the structures from the model and deteriorate the data misfit (i.e., L-curve, see detail in Hansen (1994)). Thus, due to the trade-off between the data misfit and the model perturbation, a suitable weighting parameter needs to be chosen by trial and error.

In order to deliver useful information, not only the resulting models are interesting, but also uncertainty and resolution of the obtained models are important. In our procedure formal error estimates of the velocity models cannot be computed. Therefore, this has to be achieved in different ways, e.g., via checkerboard test, spike test. Whatever method is used for resolution test, the resulting model parameters through inversion combined with the resolution tests and hypocentral uncertainties could be effectively used to interpret the final-model results. Possible trade-off between velocity structure and hypocentral parameters need also to be analyzed with various tests. Details on using the LET for earthquakes located on Katla volcano are presented in paper I.

5.2. Ambient Seismic Noise Tomography

The continuous interaction between lithosphere, oceanic waves, and atmosphere excites seismic waves and creates background seismic noise or ambient seismic noise. Standing waves on the ocean are created due to atmosphere perturbations; accordingly, the ocean bottom is subjected to continuous pressure changes, which results in emergence of elastic waves similar to earthquakes. The global level of background noise studied by Peterson (1993) is summarized as the Low Noise Model (LNM) and the High Noise Model (HNM). These global noise models show a non-uniform character of the background noise in frequency. Moreover, the level of noise is different spatially and temporarily, e.g., the water depth and the season can be important factors in the level of ambient noise intensity (e.g., Tanimoto and Um, 1999). Ambient noise could potentially be measured everywhere, which makes the method efficient compared to the earthquake/explosion based

methods in exploring the earth structure, as they are limited to a specific source and receiver geometry.

Ambient noise has already been used successfully in other branches of physics, e.g., acoustics (Weaver and Lobkis, 2001). In seismology, correlation based properties of random seismic noise signals were first explored by Aki (1957) to retrieve the dispersion properties of the subsurface. The idea has been developed rapidly over the last decades, so that today retrieving an approximation of Green's function from microseisms is an important tool to understand the earth interior. Shapiro and Campillo (2004) have shown that in the case of a completely random wavefield, the cross correlation of ambient seismic noise recorded between two stations approximates the Green's function of the medium between these two points. An obtained cross correlation function is a measure of similarity of two waveforms, which travel in line with the two stations, as a function of time-lag.

Ambient seismic noise mostly contains surface waves because they are generated, at least partially, by superficial sources, i.e., the atmosphere/ocean-crust interaction. Hence, cross correlation function calculated for two seismic stations at the surface is dominated by surface waves with dispersive properties (Friedrich et al., 1998; Shapiro et al., 2005). Depending on the components that we are correlating we expect to have Rayleigh and/or Love waves, which can potentially be distinguished using the polarization characteristics and the estimated group/phase velocities (Campillo and Paul, 2003). The ambient noise studies have been mostly focused on Rayleigh waves instead of Love waves, because it is thought to be more difficult to couple ocean waves with horizontal motions of the seafloor, which would make Love wave generation less efficient than that of Rayleigh waves (e.g., Stehly et al. 2006).

The resulting covariograms could be used for group- and phase-velocity dispersion measurements (Shapiro and Campillo, 2004). Different methods have been proposed to calculate phase and group velocity dispersion curves such as frequency-time analysis (FTAN) (e.g., Dziewonski et al, 1969), multiple filter analysis (Herrmann, 1973), and spectral methods (Ekström et al., 2009). Among them we have chosen the multiple filter analysis method of Herrmann (1973) in the current study, where a dispersed surface wave is presented by:

$$f(t,r) = \frac{1}{2\pi}\int_{-\infty}^{\infty} A(\omega,r)exp(-ikr + \emptyset)\exp(i\omega t)d\omega \qquad (7)$$

where r is the distance, t is the time, $\emptyset$ is the source phase, ω is the frequency, and k is the wavenumber. By applying a narrow-band Gaussian filter about a central frequency (ω_0) using $\exp(^{-\alpha\omega^2}/_{\omega_0^2})$, the filtered signal will be:

$$g(t,r) = \frac{1}{2\pi} A(\omega_0)\omega_0 \sqrt{\frac{\pi}{\alpha}} \exp(i(\omega_0 t - k_0 + \emptyset)) \exp(-\frac{\omega_0^2}{4\alpha}(t - {}^{r}/_{U_0})^2) \quad (8)$$

where the parameter α is the width of the filter and is usually chosen based on interstation distance (r). The last term of Eq.(8) is the envelop of the cross correlation function and the arrival time of group velocity (U_0) occurs at its maximum.

Phase velocity can be estimated using group velocity:

$$c = \frac{\omega_0 r}{-\varphi + {}^{\pi}/_{4} + {}^{\omega_0 r}/_{U_0} + N2\pi} \quad (9)$$

where φ is the phase term and is calculated using $\tan^{-1}(Im\ g(t_g,r)/Re\ g(t_g,r))$, where t_g is the arrival time of the group velocity.

We calculate the cross correlation function only between vertical components of each station pair, in so doing we focus on the Rayleigh wave packets. Due to the dispersive characteristics of the surface waves, the penetration depth of the travelling waves depends on wavelength, with longer wavelengths being sensitive to deeper structures than are shorter wavelengths. Since sub-surface velocity varies with depth, each frequency component of the surface-wave train propagates with different velocity. The velocity-frequency variation can be estimated from the cross correlation functions. Ultimately, the derived information is summarized in the dispersion curves and can be translated into velocity-depth variation.

2-D phase velocity maps have been obtained using dispersion measurements within the seismic network around Katla volcano. The inversion processes of producing 2-D phase velocity maps are performed by the method of Fast Marching Surface Tomography (FMST) (Rawlinson and Sambridge, 2005). FMST uses the Fast Marching Method (FMM) in a forward modeling which is followed by a subspace inversion. The process is done iteratively, similar to the other inversion procedures, to minimize data misfit to derive a reasonably simple model. As this is a non-unique problem, like most tomographic problems, damping and/or smoothing is required. The final inversion will result in 2-D phase velocity maps for each frequency range. Combining all 2-D phase velocity maps, each nodal point of the 2-D maps could be defined by a local phase velocity dispersion curve. Since the phase velocity is an integrated measure of shear velocity over depth and the relationship between phase velocity at different periods and intrinsic velocity at depth is not trivial, in fact non-linear, we need to take a further step and invert for depth as well. Accordingly, we designed a non-linear grid search scheme for this purpose to obtain the shear-wave velocity with depth. Details on the processing of ambient seismic noise data from the seismic network around Katla are presented in paper II.

5.3. Relative Earthquake Location

The location of earthquakes is one of the most important tasks in seismology, which strongly depends on the velocity structure. When applying the classic location procedures, the result is usually biased due to the (unknown) velocity distribution. Different methods have been developed to reduce the effect of velocity heterogeneities on earthquake location parameters. Some methods that are based on differencing operators have been introduced to improve location accuracy (e.g., Jordan and Sverdrup, 1981) and reduce the dependence of the velocity structure. These methods are built on the assumption that earthquakes with small hypocentral separation, recorded at a common station, will be affected similarly by velocity heterogeneities, so the difference of their travel times will not contain these effects (e.g., Waldhauser and Ellsworth, 2000; Wolfe, 2002). Though differencing operators are not able to remove the path effects in an absolute term and can only improve the relative locations between nearby earthquakes (Wolfe, 2002), the detailed information revealed in this may greatly improve our understanding on, e.g., earthquake source processes. In the so called 'relative location' methods, the distance between the events needs to be much smaller than the event-station distance and the scale length of the velocity heterogeneities to meet the assumptions made.

There are two common techniques, widely used for relative relocation of earthquakes: the master-event (e.g., Ito 1985; VanDecar and Crosson 1990) and the double-difference (DD) method (Got et al., 1994; Waldhauser and Ellsworth, 2000). The DD algorithm increases the spatial extent of the cluster that can be relocated, since it uses time delays of all possible earthquake pairs. On the other hand, in the master event approach, all events require correlating with the master event and, therefore it is more useful in locating very tight clusters. In both methods, the relative location problem could be described as following:

$$dr_k^{ij} = (t_k^i - t_k^j)^{obs} - (t_k^i - t_k^j)^{cal} \tag{10}$$

where t is the travel time, i and j are indexes of the event pair, k is the measured phase (P or S). *'obs'* and *'cal'* stand for observed and predicted data, respectively. Note that, j is equal to one in the master event location. The presented procedures minimize the difference between the observed and the calculated differential travel time through inversion:

$$e = \sum_{k=1}^{N} (dk_k^{ij})^2 = minimum \tag{11}$$

In order to compensate for the systematic errors in arrival times and for the uncertainties due to velocity heterogeneities, the relative relocation of events can be further improved by using cross correlation methods to produce dif-

ferential times. The accuracy of the measured differential times could possibly be less than the sampling interval of the waveforms (e.g., Frémont and Malone 1987). Therefore, the relative location will be highly accurate, on the order of meters to tens of meters (Waldhauser and Ellsworth 2000). This can be particularly useful when the onset of the pick is unclear, as for example for volcano related earthquakes (e.g., Got et al., 1994). The method is used in the present study and applied on the cluster of seismicity near the eastern rim of the Mýrdalsjökull glacier to: 1) compensate for manual phase-picking bias and use a consistence weight with each single phase pick based on the correlation coefficient, and 2) improve the relative locations of the events and estimate their relative uncertainty, which can provide useful information in the interpretation of the source mechanisms. Details on applying the relative location technique for the cross correlation differential times on the eastern flank seismicity of the Katla volcano are presented in paper IV.

6. Summary of Results

Here, I briefly summarize the four papers included in this thesis. The theoretical background and the methodology have been outlined in chapter 5 and will not be presented here. Each summary covers information to motivate the work, a description of the data preparation required in each step, the main results and the conclusions.

6.1. Three-Dimensional P wave Velocity Model and Seismicity Pattern

The tomographic imaging of an active volcano provides important information regarding its internal structure and physical properties. Despite the 2-D and 3-D images have been already published for Katla volcano (e.g., Guðmundsson et al., 1994; Jónsdóttir et al., 2007), very little is known about its 3-D structure. The resolution and coverage of the available models is limited and potentially a more detailed picture of Katla's plumbing system can be obtained by a denser network than hitherto has been operated in the area. Thus, from the two and a half years of data recorded by the network described in section 4, a 3-D P wave velocity model of Katla has been developed and the general seismicity pattern has been described. These are discussed in detail in Paper I.

The time of the first seismic wave arrivals and an initial velocity structure are required to perform the tomographic imaging. Phase identification and arrival time measurements are done manually using the SeisAn earthquake analysis software (Havskov and Ottemöller, 1999). Furthermore, the one dimensional (1-D) velocity model used by IMO for southern Iceland has been modified using the information from our observations, accomplishing a better fitting of the model to the data. The modified 1-D model together with the manually picked arrival times are then inverted simultaneously to investigate the 3-D P velocity structures and the earthquake hypocentral locations, using the PStomo_eq software (Tryggvason et al., 2002).

We present two cross sections of the final P wave velocity model passing through the caldera, from SSE to NNW (P1) and from WSW towards ENE (P2), along with depth slices of the model at 1.0-1.5 km, and 4.0-4.5 km depth (Figure 5). The most striking features of the model are high velocities

of 6.5 km/s beneath the perimeter of the central volcano at ~3-4 km depth below sea level (bsl), a high velocity body located beneath the caldera at 4 km depth, and a low velocity anomaly (~3.5-4.0 km/s) down to 1 km bsl beneath the caldera.

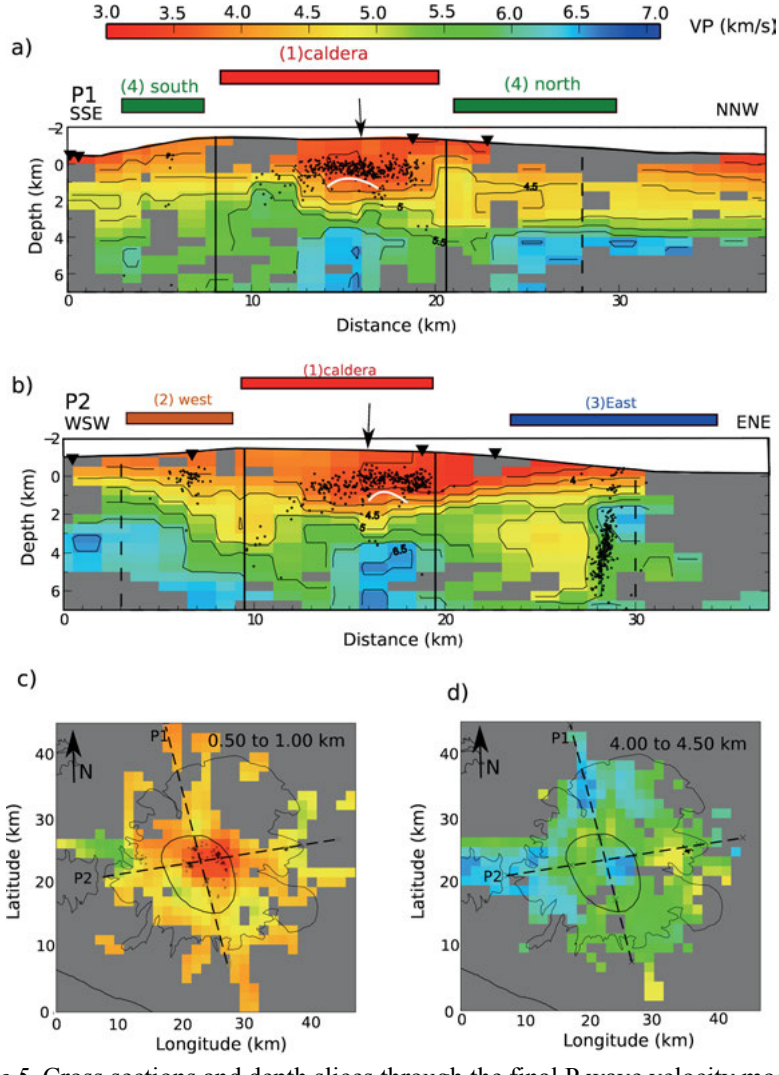

Figure 5. Cross sections and depth slices through the final P wave velocity model and the relocated seismicity. **a, b)** Cross sections. *Triangles:* stations within 3 km from the cross sections. *Black arrow*: crossing point between P1 and P2. *Vertical solid line:* Caldera rim. *Vertical stippled line:* The approximate extent of the Katla central volcano (Einarsson and Saemundsson, 1987). *White curve:* border between seismically active and non-active area. *Black dots:* relocated earthquakes within 3 km of the profiles. **c, d)** Depth slices. Stippled lines are the locations of the cross sections. The depth slices are labeled with the depth. The gray areas have no rays through them in the final iteration.

A checkerboard and hypothesis model tests are then performed in order to investigate the resolution of the obtained model to assess the results. Additionally, the absolute uncertainty of the model is estimated by propagating the data uncertainties through the inversion process (see Paper I for details).

While developing the velocity model and through the inversion process, new earthquake locations are also computed and the hypocentral parameter uncertainties are evaluated. Geographically, the earthquakes are distributed mainly in four distinct seismic clusters: 1) within the caldera, 2) west of the caldera, close to Goðabunga, 3) in the south, near Gvendarfell Rise, and 4) towards the eastern rim of the glacier, at the tip of Sandfellsjökull. According to the frequency content, each individual seismogram is characterized either as high-frequency (HF) (>5 Hz) or low-frequency (LF) (3-5 Hz) seismogram. Accordingly, each event has been classified, based on the proportion of the HF observations for each event, as VT (>75%), LP (0%) or 'Mixed' (between 0 and 75%). The earthquakes located in our resulting 3-D velocity model are shown in Figure 6, along with their associated classification (in color). Information about the active clusters is summarized in Table 3.

The caldera seismicity is more complex, with a mixture of events divided into seven sub-clusters (Figure 6a and Table 3). The distribution of the events is offset to the east of the caldera center, being shallowest in its middle, and deepening with distance to the sides. The seismicity forms a dome shape with almost only VT events at depth, a concentration of 'Mixed' events at shallow levels and a cluster of LP events at the center of the seismicity (Figure 7). We associate the base of this dome shape with a brittle-ductile transition zone and higher temperatures near the center of the caldera, where the tomographic model revealed lower velocities. This low-velocity zone, with P wave velocities in a range of 3.5-4.0 km/s down to depths of 1 km bsl, is underlain by a high-velocity core of velocities, reaching 6.5 km/s at depths of 4 km bsl. The low velocities beneath the seismogenic dome are interpreted to represent a region of concentration of hot rhyolite or rhyolitic melts, generated by fractionation of intruded magma lenses and remelting of subsiding, wet extrusives (i.e., hydrothermally altered basaltic rocks). The low velocity anomaly overlies mafic cumulates imaged as the high-velocity core at 4 km depth bsl beneath the caldera.

Our initial aim was to perform a joint inversion for both P and S wave velocities along with the hypocentral parameters as the P and S wave velocities combined (the V_P/V_S ratios) may provide diagnostic information on state variables such as temperature, porosity and pore content. However, as events with accurate enough S wave picks were few and spatially limited, estimating a stable 3-D model of S wave velocity, and consequently V_P/V_S ratios, proved difficult.

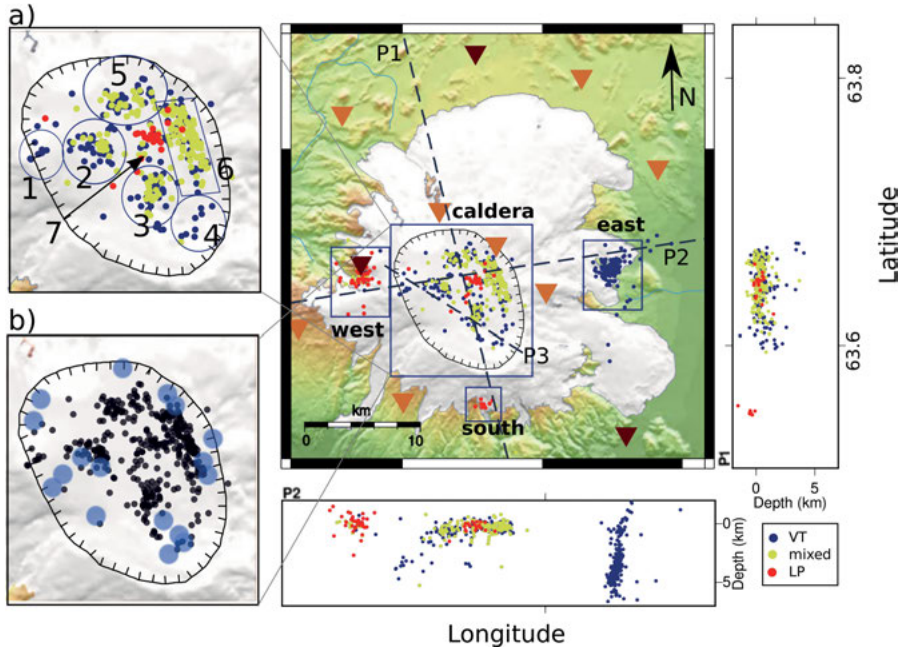

Figure 6. Classification of the relocated seismicity. Four seismogenic regions in the Mýrdalsjökull area are outlined with rectangles. VT, LP, and 'Mixed' events are shown in blue, red and yellow colors, respectively. **(a)** The caldera seismicity is mostly confined to seven small clusters, labeled 1-7. **(b)** The same seismicity map is shown with the geothermal cauldrons (blue circles). The dashed lines on the larger map represent three profiles P1-P3. The P1 and P2 cross sections show the depth distribution of the seismicity within 3km from the profiles. P3 is shown in Figure 7.

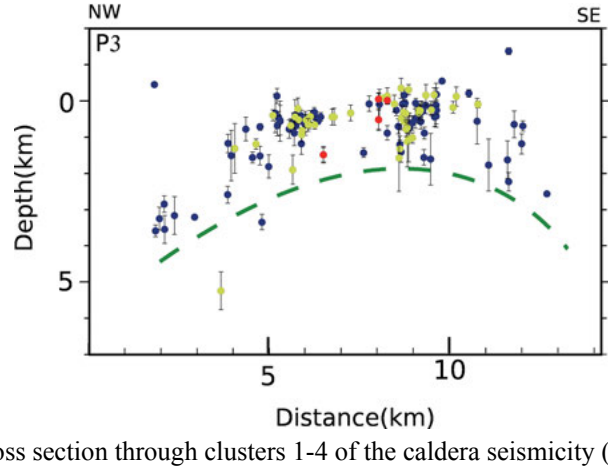

Figure 7. Cross section through clusters 1-4 of the caldera seismicity (profile P3 in Figure 6). The depth distribution of the seismicity within 2 km from the cross section is shown using the same color code as in Figure 6. The vertical bars indicate the depth uncertainty (1 σ). Dashed line shows the inferred brittle-ductile transition zone above which most seismicity occurs.

Table 3. Active source regions of the Katla volcanic system based on the earthquake located seismicity.

Active source region	Sub-cluster	Location	Event type
Caldera	Cluster 1	Caldera- western rim	VT
	Cluster 2	Caldera-towards west	Mostly VT
	Cluster 3	Caldera- centre, towards south	Mostly VT
	Cluster 4	Caldera- southeast	VT
	Cluster 5	Caldera- northern rim	Mostly 'Mixed', few LP and VT
	Cluster 6	Caldera- eastern rim	Mostly 'Mixed', few LP and VT
	Cluster 7	Caldera- centre of seismicity	LP
West	-	West of the Caldera, near Goðabunga	Mostly LP
South	-	Southern rim of the glacier, near Gvendarfell Rise	LP
East	-	Near the eastern rim of the glacier, at the tip of Sandfellsjökull	VT

6.2. Three-Dimensional Shear Wave Velocity Model

Since detailed information about the 3-D P wave velocity structure of Katla is now available, it is of interest to add constraints on the S wave velocity structure for comparison. Therefore, we apply the surface-wave tomography method using data from the same dense network of seismographs around the volcano. The ambient seismic noise tomography method has been used successfully during the last decade to evaluate the internal structure of the earth in terms of 3-D shear wave velocity. Several volcanoes have been studied with this method. First, Rayleigh waves are extracted from the high-frequency part of the secondary microseisms by correlating the vertical-component recordings at two stations. The whole process is described in detail in Paper II, including information on the preparation and processing of the continuous recordings and calculation of cross correlations. Second, phase velocity dispersion curves are measured and inverted for 2-D phase velocity maps. Finally, these maps are inverted for shear wave velocities and their variation in depth. This inversion processes is also described in detail in Paper II. An overview description is provided below.

First, hourly preprocessed seismic records are cross correlated for all possible station pairs (Figure 8a). They are then stacked into one-month covariograms. The wave trains are stable on that time scale during the entire re-

cording time for most of the station pairs. Figure 8b shows the stacked covariograms over the entire recording period in the range of 1-10 s, versus the inter-station distance.

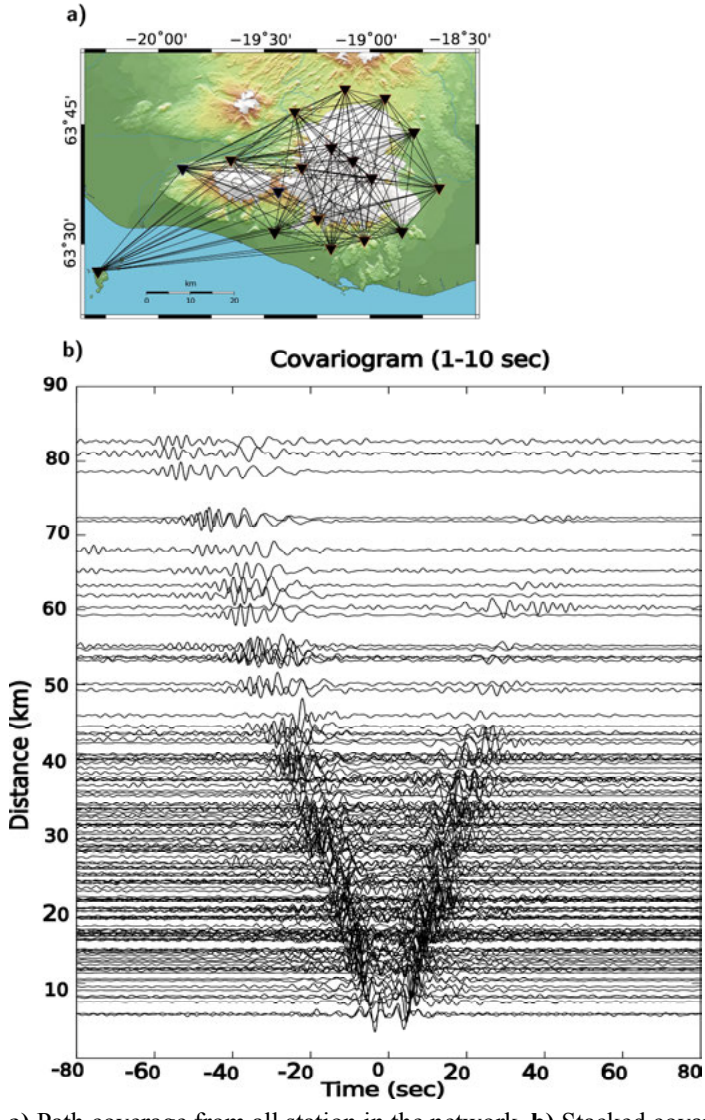

Figure 8. **a)** Path coverage from all station in the network. **b)** Stacked covariograms in the frequency range of 0.1-1 Hz for two and half years of data.

The effect of the non-uniform source distribution on phase- and group-velocity measurements for different periods and inter-station distances is estimated and the results demonstrate that the effect on group velocity is much larger than that on phase velocity. Note that the signal to noise ratio

(SNR) is used as a proxy for evaluating the energy distribution in the area. This is one reason why we choose to work with phase velocity.

Next, the phase-velocity dispersion curves are calculated for the stable covariograms and the 2-D phase velocity maps are then inverted for. The lateral resolution of the phase-velocity maps is estimated through a checkerboard test. Moreover, the absolute uncertainties of the model parameters are evaluated by propagating random noise (with standard deviation equal to the data misfit) to the final model predictions (see details in paper II). After non-linear 2-D inversion, a set of phase velocities at different periods for all local grid points is available and a local phase-velocity dispersion curve can be constructed at each point by combining them. Finally, we design a non-linear grid search inversion for shear velocity as a function of depth including a fixed ice layer at top representing the glacier of known thickness (see details in paper II).

This has resulted in a 3-D image of shear velocity to a depth of 10 km with a resolution length of 8 km in the horizontal directions (derived from checkerboard tests) and depth resolution deteriorating from 1 km near the surface to 8 km at the base of the model (derived from sensitivity kernels). Figure 9 shows two cross sections through the 3-D shear velocity model crossing the caldera in similar locations to the profiles that are presented through the P wave velocity model (see section 6.1).

We note the high velocities doming within the central volcano. A high-velocity anomaly is also clear in the cross sections of Figure 9, centered beneath the NW caldera and extending from 6 km depth bsl downward. The WE cross section has a low-velocity anomaly at 4 km depth beneath the western caldera rim. The 3-D shear-velocity model does not agree strikingly with the results of the body-wave study (see section 6.1), although some of the main features are compatible, such as the high velocities in the upper crust within the central volcano compared to its surroundings and a particularly high velocity core at 6 – 10 km depth beneath the caldera complex. We do not resolve any thin low-velocity anomaly at 2 km depth bsl as in the P wave velocity model (see section 6.1) and as suggested by Guðmundsson et al. (1994). This may be due to the limited thickness of this anomaly and the limited depth resolution in our model.

We also find anomalously high V_P/V_S ratios when we compare the average velocity depth profiles from our surface waves to the higher frequency P waves (see section 6.1). This is apparently not an artifact due to lateral refraction or topography. Instead, we argue that this discrepancy can be explained with velocity dispersion due to attenuation and a difference in frequency content, or possibly by compositional effects (to some extent).

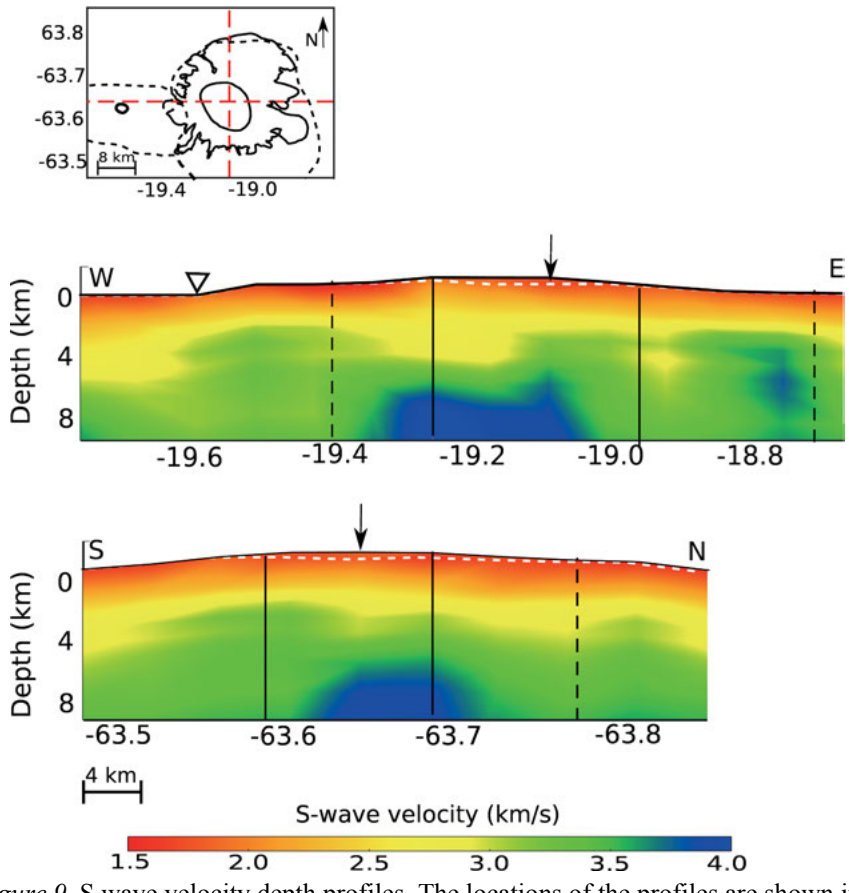

Figure 9. S wave velocity depth profiles. The locations of the profiles are shown in the top panel. The middle panel is oriented South-North and lower panel West-East as indicated. The solid black lines show where the profiles intersect the caldera, dashed black lines the outer boundary of the volcanic system. *Black arrow:* crossing points between two profiles. *Triangle:* location of Eyjafjallajökull. *White dashed line:* bottom of the ice.

6.3. Seismic Activity on the Southern Flank of Katla

In addition to the velocity structure beneath Katla, we also focus on the seismicity in the area in this study. The overall seismicity between May 2011 and August 2013 (during operation of temporary network) located in the 3-D velocity model) was presented in section 6.1. Events were divided into four active source areas two of which are well known (Caldera and Goðabunga) and the remaining two were new and were therefore the subject of further study. We focus on recorded activity on the southern flank in this section and on the eastern flank seismicity in section 6.4.

A new source region emerged on the southern flank of the Katla volcano in July 2011 during the unrest episode (see Table 1). The source region contains monochromatic LP events, and both glacial and volcanic processes can be considered as a potential source for these. Therefore, studying the characteristics of these events adds to the information not only on the mechanisms of the active seismic sources in the Mýrdalsjökull area, but also on the general knowledge of glacial covered volcanoes. Furthermore, seismic events in this area are of major interest for Katla's volcanic hazard assessment, as the coastal area south of Katla is a farming area and a popular tourist destination. In order to improve the location estimates of these events further, a complementary temporal deployment of three stations took place in 2014 in the epicentral area, and cross correlation methods were used to improve the event detection. Further analysis of the seismic sequence is carried out, in terms of waveform characteristics, temporal evolution, first motion description, and non-linear absolute event location. Paper III includes the details of this processing and the discussion regarding the activity observed in the south.

The seismicity that started on the south flank near Gvendarfell Rise in July 2011 is still active and consists of shallow, repeating LP seismic events with emergent P waves and unclear S waves (Figure 10). The southern seismic activity is characterized by small magnitudes (~ -0.5-1.2 M_L) and the frequency content is narrow banded around 3-4 Hz at the closest station (GVE) to the seismicity and nearly monochromatic around 3 Hz at most other stations. Since the similarity of waveforms is striking, a cross correlation scheme is set up between an event recorded in the IMO catalog with highest signal to noise ratio (at station ALF) and the continuous data from February 2011 to August 2013. Around 1800 events are detected with a cross correlation coefficient higher than 0.9 (mostly ≥ 0.95), significantly more compared to the 720 events of the IMO catalogue during the same time period. The southern events also occur at regular time intervals with a seasonal modulation with the highest frequency of occurrence during summer time.

The absolute locations from the IMO catalogue show a cloud of hypocenters, dispersed over a large area of several km in diameter (Figure 11), on the southern side of Mýrdalsjökull glacier, with reported uncertainties on the order of 1 km in the horizontal and several km in the vertical, suggesting that significant and variable bias due to 3-D heterogeneity is present in the locations. Thus, the best events recorded during the summer of 2014 (when 2 additional stations were deployed nearby) were relocated. The non-linear absolute location of the selected events corresponds to the outer margin of the small, fast retreating Hafursárjökull glacier (Figure 11). The relocations do not differ much from the IMO average, except that the distribution of hypocenters is much smaller than in the IMO catalog locations and the uncertainty of the relocations is around 400 m in the horizontal dimensions and 500-600 m in depth.

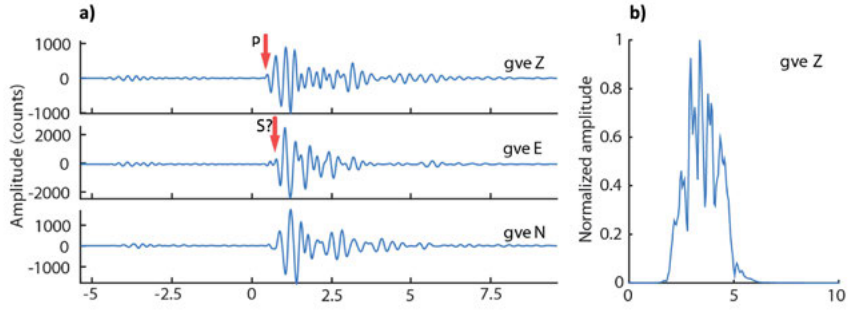

Figure 10. a) Example seismograms of an events at stations GVE. The amplitude unit is digital counts, proportional to velocity. The arrows mark the P and S wave arrivals, where identified. *b)* Normalized amplitude spectra of the Z component at stations GVE and ALF.

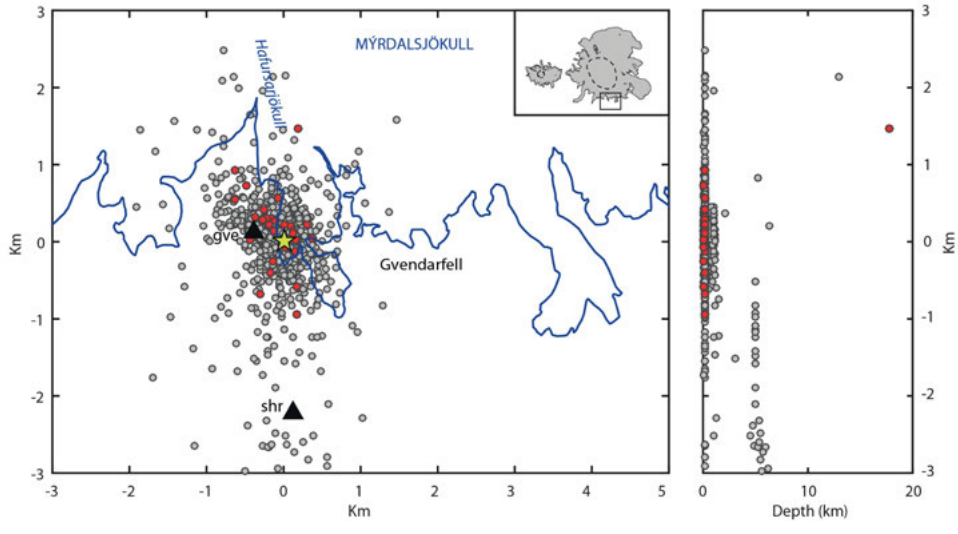

Figure 11. Locations and depth distribution of the Gvendarfell seismic events, from the IMO catalogue: *gray* = all locations 2011-2013; *red* = 30 events in summer 2014. The star is the average IMO location (N63º32.772', W19º06.588') and corresponds to the origin of the axes of the figure. Black triangles are the seismic stations. The glacier outline (in blue) is derived from LiDAR DEM obtained in 2010 (Jóhannesson et al., 2013).

The absolute depth location is not resolved well enough to be discerned from the surface, therefore a glacial origin of the Gvendarfell events, such as glacier sliding and icefalls, cannot be ruled out. However, the thickness of the ice in this area is not likely to exceed a few tens of meters. Moreover, it is unlikely that such a small glacier stream can produce such remarkably stable seismicity over years. These arguments, together with the temporal coincidence of the onset of the southern flank seismicity with the July 2011 unrest

episode, suggest that volcano-related processes are more likely than glacial to generate this seismicity. Among volcano-related processes, a hydrothermal source appears more likely than magma movement, mainly because of the marked seasonal correlation of the seismicity, which appears easier to reconcile with a source involving water. The similarity of the waveforms over a long time (at least 3.5 years) indicates a stable, non-destructive source mechanism and the regular temporal pattern suggests that the process must be controlled by a critical parameter such as a temperature-pressure condition. These features seem to be consistent with a steady process of heating and cooling (geyser-like) of a hydrothermal fluid. In this scenario, the seasonal correlation may be explained as a response to the summer ice melting that increases the water supply to the system. Therefore, it is possible that a small hydrothermal system was activated on the southern flank of Katla in coincidence with the July 2011 unrest episode. This may have been powered by either a short lived dike intrusion or a crack connection to a heat source established during the unrest. As no evidence for hydrothermal activity has been found in the area, this hydrothermal system has to be entirely concealed by the glacier or acting below the ground surface.

6.4. Seimic Activity on the Eastern Flank of Katla

A new, peculiar cluster of seismicity near the tip of Sandfellsjökull on the eastern flank of Katla volcano is analyzed in detail using data from the temporary seismic network. Several of these events are registered in the IMO catalog. The area has not been identified as a seismic source at Katla before. Therefore, studying the detail of this activity is important for volcanic hazard assessments and to further expand our knowledge on the ongoing processes of the Katla volcanic system. The Eastern events are described by their waveform characteristics, absolute and relative location, magnitudes and b-value, and their possible source mechanisms discussed (see Paper IV for details).

These events are detected owing largely to the temporary network (see section 4) that was operating between June 2011 and August 2013 in addition to the permanent network of IMO. The seismic activity is characterized as VT events with frequencies in the range of 4-25 Hz. Two families of events are identified based on their waveform similarity and clearly distinguished by differences between their amplitude ratios of P and S phases on different components (Figure 12).

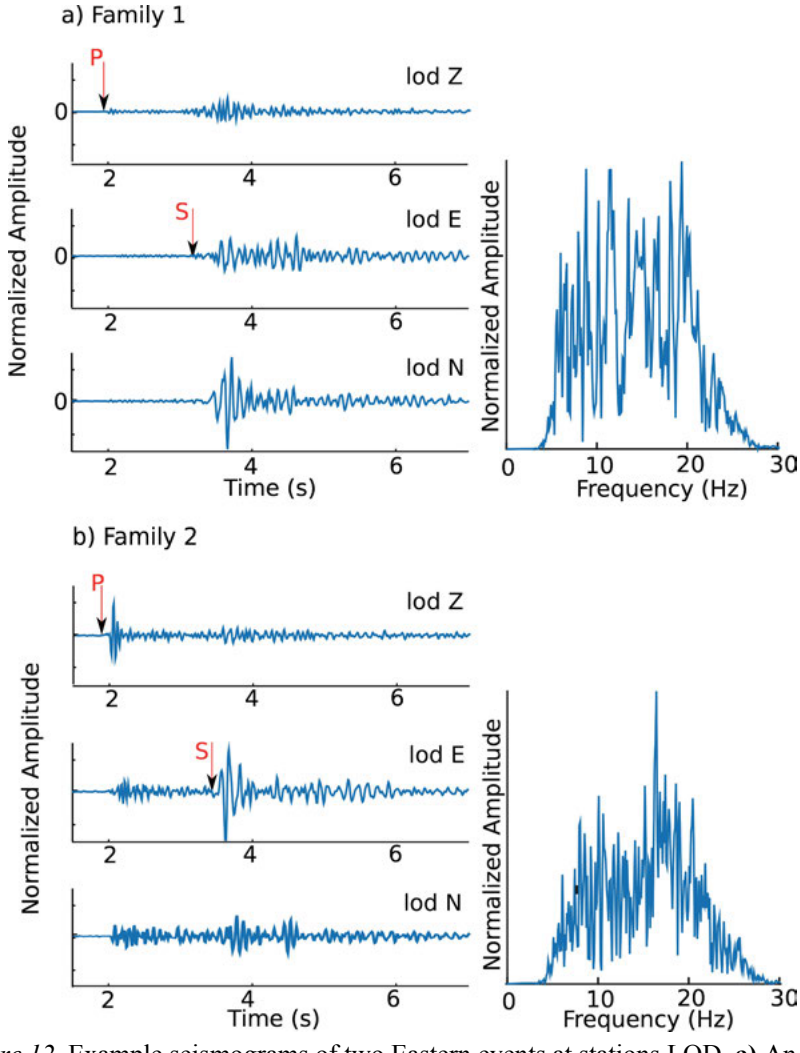

Figure 12. Example seismograms of two Eastern events at stations LOD. **a)** An example of family 1. **b)** An example of family 2. Waveforms of three components are shown to the left and their amplitude is normalized proportional to maximum amplitude of vertical component in each case. The arrows mark the P and S wave arrival times. Normalized amplitude spectra of the Z component is shown to the right.

Due to the similarity of events, a cross correlation process is applied on the continuous waveform data to improve the earthquake detection. Consequently, 300 events are found between June 2011 and August 2013. The temporary network was operating in the area during this time period and two of 9 temporary stations (KKE, LOD) were close to the Eastern activity and critical for the detection. The IMO catalog registered only 6 of these events during the same time period. Before June 2011, several events are registered in the IMO catalog, the first one in November 2001. Since the station closest to

the activity is at ~15 km distance (HVO), we are not able to improve their locations. The temporal evolution of the Eastern activity, both looking at IMO catalog and our detections, indicates a swarm-like behavior, with the two biggest swarms occurring in November 2010 and December 2011.

We locate the events using single event location and relative location (Figure 13). The relative location results show a small distribution of the cluster in all directions (~400 m) around the master event in family 1. The events of family 2 are located in a much smaller volume than family 1(~150 m). Absolute location results suggest that the master event of both families is located around 3.5 km depth.

The Eastern events' focal depths are robustly distinguished from the surface; therefore, glacial processes can be excluded as the source explanation of this seismic activity. The Eastern events are isolated in space (at 3.5 km depth in the volume of ~400 m^3 around the master event) and this clearly argues against the underlying cause being a distributed stress field in the upper crust. A local force field is more likely. A localized, cooling magma body may be oversaturated in gas and may, therefore, release pressurized gas and lower effective normal stress, which can lead to rock failure. The same holds for geothermal brine heated by a local source. This explanation may be consistent with the high b-value (1.6±0.1) that we estimated for these events. High b-values have been associated with magma transport and/or a low stress regime in volcanic regions (Roberts et al., 2015 and references therein).

In all cases, these speculations lead to a small, localized source of magma, heat or gas. But, we cannot distinguish between them. However, such a local source inevitably relates to heat, i.e., magma (directly or indirectly), which highlights the importance of the Eastern events for flank volcanism at Katla and as a consequence the associated volcanic hazard.

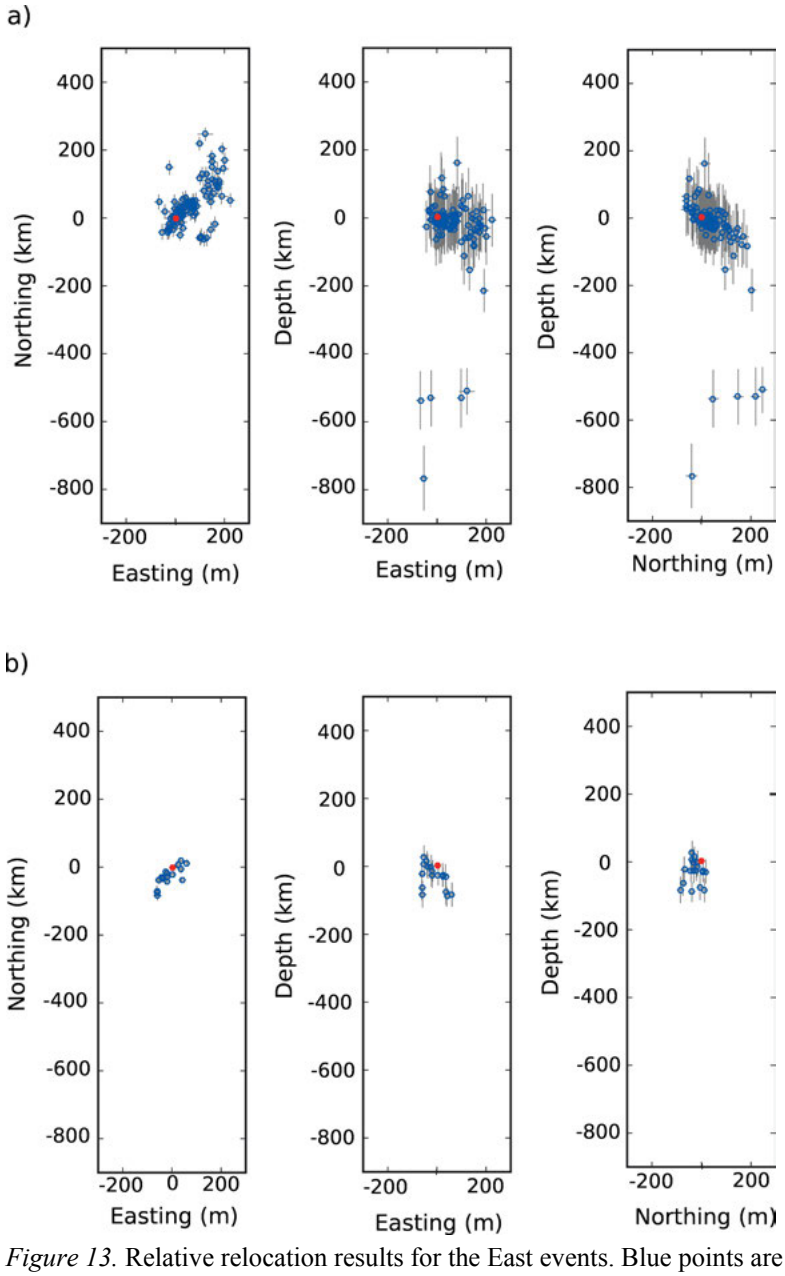

Figure 13. Relative relocation results for the East events. Blue points are the locations and grey lines represent uncertainty. The red point is the location of master event, corresponding to the origin of the axes. **a)** 132 events in family 1. **b)** 21 events in family 2.

7. Conclusions

The work in this thesis concentrates on Katla volcano in southern Iceland. The aim is to better understand the volcano's plumbing system and processes. Two techniques have been applied to study the volcano's subsurface structure, namely local-earthquake and ambient-noise tomography. These have led to images of the distribution of P wave velocity and S wave velocity within and around Katla volcano. The microearthquake activity in Katla during the two years and a half of dense observations has also been studied in detail. This has led to a detailed description of a new cluster of microearthquakes on the southern flank of the volcano and the discovery of another cluster on the eastern flank. The seismicity has been classified in terms of common volcano earthquake types (volcano tectonic and long period) and the spatial distribution of each event type described.

The P wave velocity model is based on the timing of P waves generated by local earthquakes. Their typical frequency is about 10 Hz. The S wave velocity model is based on the phase of surface waves extracted by correlation from microseismic noise measured in the frequency range between 0.2 and 0.5 Hz. The overall resolution length of both models is 4-8 km in the horizontal. Resolution differs in the vertical. In the P wave image it is highly variable, 2 km on average, but locally considerably better. In the S wave image it is more uniform, near the surface it is close to 1 km and deteriorating to 8 km at depth.

Earthquake locations are constrained both with absolute and relative methods based on measurements of absolute arrival times and differential arrival times, respectively. The uncertainty of these locations is estimated by propagating data uncertainty, assumed to equal the residual arrival times, through the location process. This results in typical uncertainties of about 300-400 m for absolute locations and considerably less for relative locations (< 100 m).

The following paragraphs summarize the main findings of the work presented in this thesis:

- ***Velocity structure:*** Even though the P wave model from body wave and the S wave model from ambient noise do not agree in detail, in part due to different resolution, the general features are consistent. The main common feature in both models is a high-velocity body beneath the caldera at depth, which is interpreted as a volume of mafic cumulates. This

high-velocity core is shifted to the west and downward in the shear-wave model compared to the P wave model. In the P wave model the anomaly is mapped at 4-6 km below which the resolution is lost. In the S wave model it is mapped below a depth of 6 km. A volume with low velocities at 2 km depth beneath the caldera was only identified in the 3-D P wave velocity model and associated with hot rhyolitic material in the shallow crust. In the S wave velocity model, which has resolution also outside the Katla volcanic system, the upper-crustal velocities are clearly higher within the volcano than outside of it. The average velocity depth profiles from surface waves on one hand and P waves on the other lead to V_P/V_S -ratio estimates that are high. This cannot be explained by lateral refraction effects, because those are accounted for by non-linear inversion. Furthermore, it is argued that this can unlikely be explained as a topographic effect. Instead, dispersion of velocity due to attenuation and a difference in frequency content can explain this anomalous feature assuming a realistic elastic quality factor of $Q_S = 25$. A high V_P/V_S ratio could possibly also be partly caused by compositional difference.

- ***Caldera seismicity:*** The seismicity of the area (here, located in the 3-D P wave velocity model) is clustered in four source regions: in the caldera region, around Goðabunga, and on the southern and eastern flanks. The events are classified as volcano tectonic, long period and 'Mixed' based on the proportion of high-frequency seismograms for each event. The distribution of the caldera events is offset to the east of the caldera center. They are shallowest in the middle, and deepen with distance to the sides. This distribution forms a dome shape with almost only volcano-tectonic events at depth, a concentration of 'Mixed' events at shallow levels and a cluster of long-period events at the center of the seismicity. This dome-shape is associated with the brittle-ductile transition zone and higher temperatures near the center of the caldera, where the tomographic model revealed low velocities. The deepest part of this low velocity region is devoid of seismicity.

- ***The southern flank seismicity:*** A new source region of monochromatic long-period events, near Gvendarfell Rise on the southern flank of Katla volcano was identified in July 2011. These events are shallow and occur at the outer margin of Hafursárjökull glacier. However, ice flow in the area is very limited, arguing against a glacial source process. A detailed study of the events characteristics, temporal evolution and locations lead us to suggest a small hydrothermal system, which was activated on the south flank of Katla in coincidence with the July 2011 unrest episode as their source.

- ***The eastern flank seismicity:*** A peculiar cluster of seismicity near the tip of Sandfellsjökull on the eastern flank of Katla volcano was detected owing largely to nearby stations in the temporary network that was operating between June 2011 and August 2013. This seismicity consists only of volcano tectonic events that occur in swarms. We cannot identify the onset of this activity because of changes in network sensitivity. Absolute locations place them at an average depth of about 3.5 km and clearly distinguish them from the surface. Relative locations concentrate most of them in a volume of ~400 m across in all directions. This seismicity cannot be associated with glacial processes, despite their proximity to Sandfellsjökull, because of their depth. They are hypothesized to be due to a small, localized source of magma, heat or gas, which cannot be distinguished.

8. Sammanfattning på Svenska

Katla är en av Islands största och i historisk tid mest aktiva vulkaner. Senast hon hade ett stort utbrott var 1918, dvs 98 år sedan. Intressant i sammanhanget är att i genomsnitt har Katla haft utbrott med 55 års mellanrum de senaste 1100 åren, och det längsta uppehållet är 100 år. Utbrottet i Katlas lillasyster, Eyjafjallajökull, 2010 var en påminnelse om att det kanske snart är dags för Katla att vakna. Jämfört med ett större utbrott i Katla var utbrottet i Eyjafjallajökull litet, tex sköts mellan två och tre gånger så mycket aska upp i atmosfären 1918 jämfört med Eyjfjallajökull 2010. Katla är belägen på södra Island under en av Islands stora glaciärer, Mýrdalsjökull, vilket gör att stora mängder smältvatten och stora isblock kan förväntas sköljas ut i havet och över jordbrukslandskapet mellan glaciären och havet vid ett större utbrott. Själva glaciären och delar av terrängen runt omkring är otillgängliga och stora delar av året helt oåtkomliga. Det förklarar delvis att relativt få studier gjorts av vulkanen.

Som en del i den särskilda forskningssatsning (SFO) som i formen av Centrum för naturkatastroflära (CNDS) som landade delvis vid Institutionen för geovetenskaper 2010-2015, gjordes flera satsningar för att bättre förstå Katla och konsekvenserna av ett större utbrott där. Den här avhandlingen är en del resultatet av det seismologiska arbetet. Island driver ett eget seismiskt nätverk med flera stationer i området kring Eyjafjallajökull och Mýrdalsjökull, med syfte att övervaka aktiviteten i vulkanerna och varna vid tecken på utbrott. Vi placerade ut ytterligare 9 stationer omkring Katla, varav tre uppe på kraterkanten där den tränger igenom glaciärisen. Syftet med de temporära stationerna var att få ytterligare data för att få säkrare bestämningar av var jordskalven sker, samt att få data ”över” att avbilda vulkanens interna struktur med. Datainsamlingen varade i 2.5 år, och den här avhandlingen beskriver arbetet, från utplaceringen och underhållet av instrumenten, databearbetningen och modelleringen, fram till och med tolkningen av resultaten.

Baserat på gångtidsdata från ungefär 850 jordskalv har jag tagit fram en tredimensionell modell av P-vågshastigheten ner till ett djup av ungefär sju km under Katla. Tekniken som använts kallas lokal jordskalvstomografi och är att likna vid skiktröntgen inom sjukvården. Gångtiderna från jordskalven används för att bestämma P-vågornas utbredningshastigheter i berggrunden. Initialt avsåg vi även göra en tomografisk S-vågsmodell, men många av jordskalven hade mycket svårtolkade S-vågor, så antalet data blev för lågt för att kunna göra det. P-vågsmodellen visar låga hastigheter centralt under den ungefär 100

km2 elliptiska kraterstrukturen ner till ett djup av ungefär 2.5 km. Under de låga hastigheterna framträder en kropp med ovanligt höga seismiska hastigheter med början på ett djup av ungefär fyra km. Utanför kratern är P-vågshastigheterna högre i de översta kilometrarna än centralt under vulkanen. P-vågsmodellen avspeglar vulkanens inre struktur, men även tillståndsvariabler som temperatur, porositet och porinnehåll. Kombinerat med en S-vågsmodell kan man börja särskilja struktur från effekterna av variationer i tillståndsvariablerna. Därför har vi utöver gångtidstomografi använt seismiskt brus för att konstruera en S-hastighetsmodell för Katla. S-vågshastigheterna fås fram genom korskorrelation av långa tidsfönster av data från två olika stationer. Maximum i korrelation antas ske vid en tidpunkt som motsvarar tidsskillnaden det tar för brus från en avlägsen källa att nå fram till de olika stationerna. Den kraftigaste komponenten i bruset består av ytvågor, vilka använts för att tomografiskt avbilda S-vågshastigheterna. Frekvensinnehållet i vågorna som används i de två olika tomografiska metoderna skiljer sig markant, vilket är en av orsakerna till att en kvantitativ jämförelse är svår, men kvalitativt visar modellerna liknande strukturer under Katla.

Bärare av information om processer och tillståndsvariabler i Katlas innandöme är även jordskalven. Deras vågformer samt var de sker ger information om de processer som är igång inuti vulkanen. Utöver de två tidigare kända områdena med omfattande seismisk aktivitet – själva kratern och ett område strax västerut – har ytterligare seismisk aktivitet (om än i mindre omfattning) i vulkanens flankområden upptäckts: strax söder om kratern och österut strax utanför glaciären. Det är svårt att avgöra vad källan för dessa jordskalv är, men möjligen kan jordskalven söderut (som sker väldigt nära ytan) kopplas till geotermisk aktivitet, och jordskalven österut som sker på ett djup av ungefär tre km kopplas till magmatiska processer. Seismiciteten inuti kratern är samlad inom ett något mindre område än själva kratern, centrerat öster om kraterns mitt, vilket kan tyda på att en ny krater håller på att bildas. Jordskalven är här väldigt grunda o sker oftast inte djupare än några få kilometer. När berget blir för varmt är det generellt sett inte tillräckligt sprött för att jordskalv ska kunna ske, utan mjukt och segt. Vi tolkar det som att området under kratern är extremt varmt och att de låga seismiska hastigheterna visar på geotermisk aktivitet. Här möter också våt och omvandlad basalt hetare magma som injicerats från djupare delar av vulkansystemet, i slutändan ända nerifrån manteln. De våta och omvandlade basalterna smälter eftersom de har en lägre smältpunkt än magman som kommer nerifrån. De höga hastigheterna som syns i båda tomografiska modellerna nedanför de låga hastigheterna tror vi utgörs av tunga mafiska bergarter som separeras ur smältan när magman svalnar, alternativt när den ryolitiska magman bildas. Sammantaget visar det på att Katla inte kan förväntas sova särskilt djupt, då processer som involverar både smälta och väldigt höga temperaturer pågår i ett område som inte är särskilt långt under ytan. Mitt arbete i den här avhandlingen har bidragit till att förstå dessa processer och att kartlägga var i vulkansystemet de sker.

9. Acknowledgements

Since the beginning of my studies at Uppsala University, I have experienced a lot of adventures, which traveling to Iceland on 3rd day of my PhD was the most memorable one. I never thought that it takes 3 hours flight to reach Iceland and landing in this amazing island gave me somehow the feeling of being astronaut landed on Mars. This feeling was getting stronger and stronger, when I went for the first time to Katla to install a seismic station! My childhood dreams of going to space came true by this trip! Particularly, when Greg was calling me 'Jedi'.

This thesis would not have been finished without a number of people contributing and supporting me along the way. I am especially grateful for all those have been involved in this study, those who made my life in Uppsala more comfortable and happy and those **who I might forget to mention**.

First and foremost, I would like to thank my supervisors for their guidance, encouragement, inspiration and valuable support. Ari, thanks for giving me the possibility to do this research and supporting me through this journey. Oli, thanks for all your patience and encouragement. I will be always more than grateful for all the things you have thought me.

I am thankful to Samar, who welcomed me and shared her office with me during the first days in Uppsala. Samar, I cannot stop laughing, when I am thinking about the time we were having seismology together as teacher assistant. When I arrived in Uppsala it was maybe the worst time of the year, mid October. Zara and Peggy, it was impossible for me to pass through the first year without your help. Zara, your emails, while I was alone during Christmas time in Uppsala made me so happy. Peggy, you gave me a lot of confidence to stay and continue, du var inte bara min svenskalärare, men också en underbar snäll vän. I am especially grateful to Oli and Bea for taking care of me while I faced some health problems; I felt that I have a second family in Uppsala. I also appreciate Maryeh and Omid; and Sahar and Reza, for all the nights that I spend with them during first two years.

Giulia, I am so glad that I shared this journey with you, our friendship has enlightened the road ahead, and it would not have been the same without you. If I need to thank Katla, I will definitely do only for this specific friendship and amazing 'GZ' program! Aggela, thanks for always being my friend, it means a lot to me. Thanks for all the supports that you gave me especially during the last year. Giulia and Aggela, I don't know the 'absolute' amount of thank that I owe you, but at least I thank you in a 'relative sense'!!! A

special thank to Claudia who I shared my office with during the last years and who was always helpful and open for discussion. Claudita, I will miss our historical, sociological, political and all non-scientific discussions, particularly on food part, you and Oscar are the best 'pataconerare'! Darina and Karin, I will miss all the moments that we shared during lunch. We should definitely go for another 'bet' after my defense and this time hot sauna for Karin as punishment! Sissa, I am so happy for sharing some time with you. I fell in love with your idea about pet-therapy cafe! Thanks for all the cutest pictures ever that you have left for me. Joanna, thanks for being such an amazing accompany in the adventure of dark forests in northern Sweden. Mahboubeh and Suman, such a great day we had in adventurebana-Fjälnora, even though I screamed a lot, but I enjoyed very much of that day.

Frederic and Ka Lok, I won't forget the field trip to Iceland and all the roaming around roads without map!!! You two healthy guys, I never understand how one can prefer yogurt to ice-cream! Frederic, thanks to being always kind and helpful specially during the first years for helping with data conversion.

Björn, you were the first person I have met from my Uppsala family, in Vienna, before my PhD starts. That was an incredibly friendly interview and made me too eager to arrive to Uppsala. Thanks for all the supports I have get from you while working with SIL system and correlation program and many other things. Special thank also goes to Karin, Hamzeh and Darina for helping me with picking with amazing Lokimp! I also thank Joanna, Claudia, Karin and Oli for accompany me in picking exercises. Eva, many thanks for helping to run correlation program. Thanks to Hossein, Hamzeh, Asdis and Taghi shirzad for all the useful discussions on ambient noise processes. I also thank David, Adam, Bjarne, Valentine, Sophie, and Steffi for useful discussions. I also owe a great thank to Iwona for helping with calculation in Perple-X. Thanks Damon for all help with graphics. Big thank to Aggela, Darina, Frederic, Claudia, and Rebekka for reading through the thesis draft, this wouldn't be the same without you. Thanks to Ari and Oli to polishing the last draft of the thesis and also to all my coauthors.

This thesis wouldn't have been existed without financial support of Central Natural Disaster Science (CNDS). To my CNDS family, I am happy for being part of this group. Specially to Diana, Jean-marc, Colin and Edvardo, for all joyful moments in Swedish course. Thanks also to Sussane, Viveca and Atena for all their support when I introduced to CNDS.

Special thanks go to Arnud and Michael for all the technical assistance. Arnua, thanks for all your friendly helps when I have just arrived in Uppsala. Also thanks to Michael as my officemate during the first years. Taher have a special place here for supporting and helping with everything. I also would like to thank all the administration staff for being always helpful.

I am very grateful to Oli, Laust, Chris and Roland for all the things that I have learned in their lectures. Among all, I cannot skip to thank Yusef Shar-

ghi who was my bachelor supervisor and made me interested in geophysics, as well as Mohammad Tatar who supervised me during my master. Thanks for all the things I have learned from you. You made me sure about my choice to study earthquake seismology! I also owe a great thanks to Hossein, who had always an open door and helped a lot not only when I was in Iran, but also during my whole PhD time.

To all the people that made my personal life in Uppsala very enjoyable. Saba, Chiara, and Soroor, thank to sharing a lot of joyful moments. Sahar, Reza and Arad; Fatemeh, Hamzeh and Haniyeh; Sophie and Behrooz; Darya and Reza thanks for being like my family in Uppsala. Mahnaz, even though you were not here in Uppsala, all your supports from Iran means a lot to me.

At the end, my deepest gratitude goes to my entire family, especially my parents, who supported me during the entire time. Simply, I cannot find any words to thank them as much as they support me! 'Başiniza dolanaram, ömür boyu sağ yaşayin'. Also to Eshrat, my mother-in-law, being very kind and helpful particularly during the last weeks feeding me with amazing food, otherwise I wouldn't survive!

Arash, thanks for being here! Thanks for being so kind. Second half of my stay in Uppsala was definitely way happier than the first two years. It was impossible to make this journey to the end without you. Thanks for all the things you have done for me and your help and support during all those years! 'Dostet daram azizam'

10. References

Aki, K., 1957. Space and time spectra of stationary stochastic waves, with special reference to microtremors, Bull. Earthq. Res. Inst., 35, 415–457.

Aki, K., Christoffersson, A., and Huseby E.S., (1974). Determination of the three-dimensional seismic structure of the lithosphere, J. Geophys. Res., 82, 277-296.

Árnadóttir, T., Lund, B., Jiang, W., Geirsson, H., Björnsson, H., Einarsson, P., and Sigurdsson, T., (2009). Glacial rebound and plate spreading: Results from the first countrywide GPS observations in Iceland, Geophys. J. Int., 177 (2), 691-716. doi: 10.1111/j.1365-246X.2008.04059.x.

Bjarnason, I.Th., Menke, W., Flóvenz, Ó.G., and Caress, D., (1993). Tomographic image of the Mid-Atlantic plate boundary in southwestern Iceland, J. Geophys. Res., 98(B4), 6607-6622. doi:10.1029/92JB02412.

Bjarnason, I.T., Wolfe, C.J., Solomon, S.C., Gudmundsson, G., (1996). Initial results from the ICEMELT experiment: body-wave delay times and shear-wave splitting across Iceland, Geophys. Res. Lett. 23, 459–462.

Bjarnason, I., T., (2008.) An Iceland hotspot saga, Jökull, 58, 3-16.

Björnsson, H., (1975). Subglacial water reservoirs, jökulhlaups and volcanic eruptions, Jökull, 25, 1-14.

Björnsson, H., Pálsson, F., and Guðmundsson, M.T., (2000). Surface and bedrock topography of Mýrdalsjökull, Iceland, the Katla caldera eruptions sites and routes of jökulhlaups, Jökull, 49, 29-49.

Björnsson, H., and Pálsson, F., (2008). Icelandic glaciers, Jökull, 58, 365-368.

Budd, D.A., Troll, V.R., Dahren, B., and Burchardt, S., (2016a). Persistent multi-tiered magma plumbing beneath Katla volcano, Iceland. Geochem. Geophys. Geosys., doi:10.1002/2015GC006118.

Campillo, M. and Paul, A., (2003). Long-range correlations in the diffuse seismic
coda, Science, 299, 547–549.

Caricchi, L., and Blundy, J., (2015). The temporal evolution of chemical and physical properties of magmatic systems, Gological Society, London, Special Publication, 422, 1-15.

Carmichael, I. S. E., (1964). The petrology of Thingmuli, a Tertiary volcano in eastern Iceland, J. Petrol. 5, 435-460.

Crosson R.S., (1976). Crustal structure modeling of earthquake data: 1. Simultaneous least squares estimation of hypocenter and velocity parameters, J. Geophys. Res. (Solid Earth and planets), 81, 3036-3046.

DeMets, C. G., Gordon, R., Argus, D. F., and Stein, S., (1994). Effect of recent revisions to the geomagnetic reversal time scale on estimates of current plate motions, Geophys. Res. Lett., 21, 2191-2194.

Dziewonski, A., Bloch, S., and Landisman, M., (1969). A technique for the analysis of transient seismic signals, Bull. Sesi. Soc. Am., 59(1), 47-444.

Einarsson, P., (1991). Earthquakes and present-day tectonism in Iceland, Tectonophysics, 189(1-4), 261-279. doi:10.1016/0040-1951(91)90501-I.

Einarsson, P., (2000). Events associated with the jökulhlaup in Jökulsa a Solheimasandi in July 1999 (in Icelandic). The Geoscience of Iceland , meeting on the Eyjafjallajökull and Myrdalsjökull unrest in 1999. Abstract volume P.14.

Einarsson, P., and Brandsdóttir B., (2000). Earthquakes in Mýrdalsjökull area, Iceland, 1978-1985: seasonal correlation and connection with volcanoes, Jökull, 49, 59-74.

Einarsson, P., and Hjartardóttir, A.R., (2015). Structure and tectonic position of the Eyjafjallajökull volcano, S-Iceland, Jökull, 65, 1-16.

Einarsson, P., and Sæmundsson K., (1987). Earthquake epicenters 1982-1985 and volcanic systems in Iceland, In: Í hlutarins eðli: Festschrift for þorbjörn Sigurgeirsson, edited by þ. Sigfússon, Menningarsjóður, Reykjavík.

Einarsson, P., Soosalu, H., Sturkell, E., Sigmundsson F., and Geirsson, H., (2005). The activity at the central volcano Katla and its vicinity since 1999 and possible scenarios (in Icelandic), In: Evaluation of Risk Due to Volcanic Eruption in Western Mýrdalsjökull and Eyjafjallajökull, (Eds. Guðmundsson, M.T. and Gylfason, Á.G.), University Press, Reykjavík, Iceland, 151-158.

Ekstrom, G., Abers, G.A., and Webb, S.C., (2009). Determination of surface-wave phase velocities across USArray from noise and Aki's spectral formulation, Geophys. Res. Lett., 36(18), L18301.

Frémont, M.J. and Malone, S.D., (1987). High precision rela¬tive locations of earthquakes at Mount St. Helens, Wash¬ington, J. Geophys. Res., 92(B10), 10223–10236.

Friedrich, A., Krüger, F., and Klinge, K., (1998). Ocean-generated microseismic noise located with the Gräfenberg array, J. Seismol., 2, 47–64.

Got, J.-L., Fréchet, J. and Klein, F.W., (1994). Deep fault plane geometry inferred from multiplet relative relocation beneath the south flank of Kilauea, J. Geophys. Res., 99(B8), 15375–15386.

Gudmundsson, O., (2003). The dense root of the Iceland crust, Earth Planet, Sci. Lett., 206(3-4), 427-440, doi:10.1016/S0012-821X(02)01110-X.

Guðmundsson, O., Brandsdóttir, B., Menke, W., and Sigvaldason, G.E., (1994). The crustal magma chamber of the Katla volcano in south Iceland revealed by 2-D seismic undershooting, Geophys. J. Int., 119(1), 277-296. doi:10.1111/j.1365-246X.1994.tb00928.x.

Guðmundsson, O., Khan, A., and Voss, P., (2007). Rayleigh-wave group-velocity of the Icelandic crust from correlation of ambient seismic noise, Geophys. Res. Lett., 34(14), L14314.

Hansen, P.C., (1994). Regularization tools: A Matlab package for analysis and solution of discrete ill-posed problems, Numerical Algorithm, 6(1),1-35.

Havskov, J., and Ottemöller L., (1999). SeisAn Earthquake analysis software, Seis. Res. Lett., 70, 532-534.

Herrmann, R.B., (1973). Some aspects of band-pass filtering of surface waves, Bull. Seismol. Soc. Am., 63, 663–671.

Ito, A., (1985). High resolution relative hypocenters of similar earthquakes by cross-spectral analysis method, J. Phys. Earth., 33, 279–294.

Jakobsson, S.P., (1979). Petrology of Recent basalts of the Eastern Volcanic Zone, Iceland, Acta Naturalia Islandica, 26, 1-103.

Jordan, T.H., Sverdrup, K.A., (1981). Teleseismic location techniques and their application to earthquake clusters in the south-central Pacific, Bull. Seismol. Soc. Am., 71(4),1105–1130.

Jónsdóttir, K., Tryggvason, A., Roberts, R., Lund, B., Soosalu, H., and Bödvarsson, R., (2007). Habits of glacier covered volcano: seismimicity and structure study of the Katla volcano, south Iceland, Ann. Glaciol., 45(1), 169-177. doi:10.3189/172756407782282499.

Jóhannesson, T., Björnsson, H., Magnússon, E., Guðmundsson, S., Pálsson, F., Sigurðsson, O., Thorsteinsson, T., Berthier, E., (2013). Ice-volume changes, bias estimation of mass-balance measurements and changes in subglacial lakes derived by lidar mapping of the surface Icelandic glaciers, Ann. Glaciol. 54(63), 63–74. doi:10.3189/2013AoG63A422.

Jónsdóttir, K., Roberts, R., Pohjola, V., Lund, B., Shomali, Z.H., Tryggvason, A., and Bödvarsson, R., (2009). Glacial long period seismic events at Katla volcano, Iceland, Geophy. Res. Lett., 36, L1140. doi: 10.1029/2009GL038234.

Lacasse, C., Sigurdsson, H., Johannesson, H., Paterne, M., and Carey, S., (1995). Source of ash zone 1 in the North Atlantic. Bull. Volcanol. 57, 18–32.

Lacasse, C., Sigurdsson, H., Carey, S.N., Jóhannesson, H., Thomas, L.E., and Rogers, N.W., (2007). Bimodal volcanism at the Katla subglacial caldera, Iceland: Insight into the geochemistry and petrogenesis of rhyolitic magmas. Bull. Volcanol. 69(4), 373-399. doi:10.1007/s00445-006-0082-5.

LaFemina, P., Dixon, T.H., Malservisi, R., Arnadottir, T., Sturkell, E., Sigmundsson, F., and Einarsson, P., (2005). Geodetic GPS measurements in south Iceland: Strain accumulation and partitioning in a propagating ridge system, J. Geophys. Res., 110(B11), B11405. doi: 10.1029/2005JB003675.

Larsen, G., (1994). Súr og basísk gjóskulög frá Kötlu - er gossaga síðustu 1000 ára dæmigerð fyrir eldstöðina? In: Kötlustefna, 26. februar 1994:4-5. (Ed. M. T. Guðmundsson), Jarðfræðafélag, Íslands, Reykjavík.

Larsen, G., (2000). Holocene eruptions within the Katla volcanic system, Iceland: Notes on characteristics and environmental impact. Jökull, 48, 1-28.

Larsen, G., Newton, A.J., Dugmore, A.J., and Vilmundardottir, E.G., (2001). Geochemistry, dispersal, volumes and chronology of Holocene silicic tephra layers from the Katla volcanic system, Iceland, J. Quarter. Sci., 16(2), 119-132.

Menke, W., (1986). Geophysical data analysis: Discrete inverse theory (rev. ed.), International Geophysics Series, 45, Academic Press Inc.

Meyer, P.S., Sigurdsson, H., Schilling, J.G., (1985). Petrological and geochemical variations along Iceland's Neovolcanic zones. J. and Geophys. Res., 90(B12), 10043-10072.

Óladóttir, B.A., Sigmarsson, O., Larsen, G., and Thordarson, T., (2008). Katla volcano, Iceland: Magma composition, dynamics and eruption frequency as recorded by Holocene tephra layers. Bull. Volcanol. 70(4), 475-493. doi: 10.1007/s00445-007-0150-5.

Óskarsson, N., Steinthorsson S., and Sigvaldson G.E., (1985). Iceland geochemical anomaly: origin, volcanotectonics, chemical fractionation and isotope evolution of the crust, J. Geophys. Res., 90(B12), 10011-10025. doi: 10.1029/JB090iB12p10011.

Paige, C.C., and Saunders, M.A., (1982). LSQR: An algorithm for sparse linear equations and sparse least squares. ACM. Trans. Math. Softw., 8(2), 195-209. doi:10.1145/355984.355989.

Pavlis, G.L. and Booker, J.R., (1980). The mixed discrete-continuous inverse problem: Application to the simultaneous determination of earthquake hypocentres and velocity structure, J. Geophys. Res., 85, 4801–4810.

Pedersen, R., and Sigmundsson F., (2006). Temporal development of the 1999 intrusive episode in the Eyjafjallajökull volcano, Iceland derived from InSAR images. Bull. Volcanol., 68(4), 377-393. doi:1 0.1007/s00445-005-0020-y.

Peterson, J., (1993). Observations and modeling of seismic background noise, US geological survey, open-file report, 93-322.

Pinel, V., Sigmundsson, F., Sturkell, E., Geirsson, H., Einarsson, P., Guðmundsson, M.T., Högnadóttir Þ., (2007). Discriminating volcano deformation due to magma movements and variable surface loads: application to Katla subglacial volcano, Iceland, Geophysical J. Int,. 169, 325-338, doi: 10.1111/j.1365 246X.2006.03267.x.

Pálmason, G. (1971). Crustal structure of Iceland from explosion seismology, Ph.D. thesis, 187 pp., Vésindafélag Isl. Rit, 40, Reykjavék, Iceland.

Pálmason, G., (1980). A continuum model of crustal generation in Iceland; Kinematic aspects, J. Geophys., 47, 7-18.

Rawlinson, N., and Sambridge, M., (2005). The fast marching method: an effective tool for tomographic imaging and tracking multiple phases in complex layered media, Expl. Geophys., 36, 341–350.

Scharrer, K., Spieler, O., Mayer, Ch., and Munzer, U., (2008). Imprints of subglacial volcanic activity on a glacier surface—SAR study of Katla volcano, Iceland, Bull. Volcanol., 70, 495-506. doi:10.1007/s00445-007-0164-z.

Sgattoni, G., (2016). Characteristics and geological origin of earthquakes and tremor at Katla volcano (S-937 Iceland), Ph.D. thesis, 136 pp., University of Bologna, Bologna, Italy and University of Iceland, Reykjavik, Iceland.

Shapiro, N.M., Campillo, M., Stehly, L., and Ritzwoller, M.H., (2005). Highresolution surface-wave tomography from ambient seismic noise, Science, 307(5715), 1615–1618.

Shapiro, N.M., and Campillo, M., (2004). Emergence of broadband Rayleigh waves from correlations of the ambient seismic noise, Geophys. Res. Lett., 31(7), L07614.

Sigmundsson, F., (2006). Iceland Geodynamics: Crustal Deformation and Divergent Plate Tectonics, Praxis Publishing.

Sigurdsson, O., Zophonıasson, S., and Isleifsson, E., (2000). The jökulhlaup from Solheimajökull July 18th 1999 (Jökulhlaup ur Solheimajökli 18. julı 1999, in Icelandic with English summary), Jökull, 49, 75 – 80.

Soosalu, H., Jónsdóttir K., and Einarsson, P., (2006). Seismicity crisis at the Katla volcano, Iceland: signs of a cryptodome?, J. Volcanol. Geotherm. Res., 153(3-4), 177-186. doi:10.1016/j.jvolgeores.2005.10.013.

Spaans, K., Hreinsdöttir, S., Hooper, A., and Ófeigsson, B.G., (2015). Crustal movement due to Iceland's shirinking ice caps mimic magma inflow signal at Katla volcano. Sci. Rep., 5, 10285. doi:10.1038/srep10285.

Stefánsson, R., Böðvarsson, R., Slunga, R., Einarsson, P., Jakobsdóttir, S., Bungum, H., Gregersen, S., Havskov, J., Hjelme J., and Korhonen, H., (1993). Earthquakes prediction research in the South Iceland seismic zone and SIL project, Bull. Seismol. Soc. Am., 83(3), 696-716.

Stehly, L., Campillo, M. and Shapiro, N.M., (2006). A study of the seismic noise from its long-range correlation properties, J. Geophys. Res., 111, B10306.

Sturkell, E., and Sigmundsson, F., (2003). Recent unrest and magma movement at Eyjafjallajökull and Katla volcanoes, Iceland, J. Geophys. Res., 108, B82369. doi:10.1029/2001JB000917.

Sturkell, E., Einarsson, P., Roberts, M.J., Geirsson, H., Guðmundsson, M.T., Sigmundsson, F., Pinel, V., Guðmundsson, G.B., Ólafsson, H., and Stefánsson, R., (2008). Seismic and geodetic insights into magma accumulation at Katla subglacial volcano, Iceland: 1999 to 2005. J. Geophys. Res.,113(B03212). doi: 10.1029/2006JB004851.

Saemundsson, K., (1978). Fissure swarms and central volcanoes of the neovolcanic zones ofIIceland, Geol. J. Spec. Iss. 10, 415–432.

Tanimoto, T. and Um, J., (1999). Cause of continuous oscillations of the Earth, J. Geophys. Res., 104(B12), 28723-28739. doi: 10.1029/1999JB900252.
Thorarinsson, S., (1975). Katla og annall Kotlugosa. Árbók Ferðafélags Íslands, Reykjavık, 125–149.
Thordarson, T., and Larsen, G., (2007). Volcanism in Iceland in historical time: Volcano types, eruption styles and eruptive history, J. Geodynamics, 43(1), 118-152.
Thurber, C.H., (1983). Earthquake locations and three-dimensional crustal strauctures in the Coyote lake area, Central California, J. Geophys. Res., 88(B10), 8226-8236.
Tryggvason, E., (1973). Seismicity, earthquake swarms and plate boundaries in the Iceland region, Bull. Seismol. Soc. Am., 63(4), 1327-1348.
Tryggvason, A., Rögnvaldsson, S.T., and Flóvenz O.G., (2002). Three dimensional imaging of the P- and S-wave velocity structure and earthquake locations beneath southwest Iceland, Geophys. J., Int., 151(3), 848-866. doi:10.1111/j.1365-246X.2006.02925.x.
VanDecar J.C., and Crosson R.S., (1990). Determination of teleseismic relative phase arrival times using multi-channel cross-correlation and least squares, Bull. Seism. Soc. Am., 80(1), 150-169.
Waldhauser, F., and Ellsworth, WL., (2000). A double-differ¬ence earthquake location algorithm; method and application to the northern Hayward Fault, California, Bull. Seism. Soc. Am., 90, 1353–1368.
Weaver, R.L., and Lobkis, O.I.,. (2001). Ultrasonics without a source: Thermal fluctuation correlations and MHz frequencies, Phys. Rev. Lett., 87, 134301
Wolfe, C.J., (2002). On the Mathematics of Using Difference Operators to Relocate Earthquakes. Bull. Seis. Soc. Am., 92(8), 2879-2892. doi: 10.1785/0120010189.
Wolfe, C.J., Bjarnasson, I.Th., VanDecar, J.C., and Solomon, S.C., (1997). Seismic structure of the Iceland mantle plume, Nature, 385, 245-247.

Acta Universitatis Upsaliensis

Digital Comprehensive Summaries of Uppsala Dissertations from the Faculty of Science and Technology 1430

Editor: The Dean of the Faculty of Science and Technology

A doctoral dissertation from the Faculty of Science and Technology, Uppsala University, is usually a summary of a number of papers. A few copies of the complete dissertation are kept at major Swedish research libraries, while the summary alone is distributed internationally through the series Digital Comprehensive Summaries of Uppsala Dissertations from the Faculty of Science and Technology. (Prior to January, 2005, the series was published under the title "Comprehensive Summaries of Uppsala Dissertations from the Faculty of Science and Technology".)

Distribution: publications.uu.se
urn:nbn:se:uu:diva-303342

ACTA
UNIVERSITATIS
UPSALIENSIS
UPPSALA
2016